Copyright Warning & Restrictions

The copyright law of the United States (Title 17, United States Code) governs the making of photocopies or other reproductions of copyrighted material.

Under certain conditions specified in the law, libraries and archives are authorized to furnish a photocopy or other reproduction. One of these specified conditions is that the photocopy or reproduction is not to be "used for any purpose other than private study, scholarship, or research." If a, user makes a request for, or later uses, a photocopy or reproduction for purposes in excess of "fair use" that user may be liable for copyright infringement,

This institution reserves the right to refuse to accept a copying order if, in its judgment, fulfillment of the order would involve violation of copyright law.

Please Note: The author retains the copyright while the New Jersey Institute of Technology reserves the right to distribute this thesis or dissertation

Printing note: If you do not wish to print this page, then select "Pages from: first page # to: last page #" on the print dialog screen

ABSTRACT

This study investigates the performance of a 1-inch long 4-vane open impeller centrifugal pump under two phase flow conditions. The paddle wheel pump, as branded by its manufacturer the Worthington Corporation, had a specific speed of 3400 (based on gallons per minute, feet of water and revolutions per minute) corresponding to a 7-inch impeller diameter. A 1/8-inch perforated steel pipe carried the compressed air to within four inches of the impeller eye where the air was injected into the water stream (See figures 18 and 20).

The three variable inputs were, water flow rate, pump speed and air flow rate. The output parameters measured were discharge, suction pressure, and torque. While measuring the output parameters, various combinations of the input variables were employed in order to find the maximum air-water volumetric ratio at which water flow stopped and the discharge head dropped to zero.

At the pump speeds and air flow rates ranging from 1500 RPM to 3500 RPM and from 1.72×10^{-3} cubic feet/second

to 2.65×10^{-3} cubic feet/second respectively, it was found that increasing the water flow rate from zero capacity to a certain limit resulted in an increase of the discharge head (See figures 1 to 5). This limiting capacity varied from 40 to 60 per cent of the pump's design capacity (35 GPM at 3550 RPM and 220 feet of water). A further increase of the water flow rate beyond the limiting capacity resulted in a quick drop of the discharge head. This characteristic behavior of the head-capacity curve was particularly noticeable at the higher air flow rates which ranged from 1.72×10^{-3} cubic feet/second to 2.65×10^{-3} cubic feet/second. It was also observed that at a given pump speed, increasing the volumetric air flow rate caused the head-capacity curve to peak at a lower discharge pressure. Finally, increasing the air content caused a shift in the efficiency curves such that peaked at a lower efficiency value as well as a lower flow capacity.

THE EFFECTS OF AIR-WATER TWO PHASE FLOW ON THE PERFORMANCE OF A CENTRIFUGAL PUMP

BY

KARNIG EKIZIAN

A THESIS

PRESENTED IN PARTIAL FULFILLMENT OF

THE REQUIREMENTS FOR THE DEGREE

OF

MASTER OF SCIENCE IN MECHANICAL ENGINEERING

AT

NEWARK COLLEGE OF ENGINEERING

Newark, New Jersey
1968

APPROVAL OF THESIS

THE EFFECTS OF AIR-WATER TWO PHASE FLOW ON THE PERFORMANCE OF A CENTRIFUGAL PUMP

BY

KARNIG EKIZIAN

FOR

DEPARTMENT OF MECHANICAL ENGINEERING

NEWARK COLLEGE OF ENGINEERING

BY

FACULTY COMMITTEE

APPROVED: _____

_____

_____

NEWARK, NEW JERSEY

JUNE, 1970

PREFACE

This study was performed to determine the effect of injecting a variable amount of compressed air into the water stream prior to introduction into the impeller eye of a 1-inch open impeller centrifugal pump. The effects of air content and pump speed on the discharge head and pump efficiency were tested. In addition, the optimal two-phase flow parameters were determined and compared with the no-air flow parameters.

Literature on the subject of two-phase flow is extensive in regard to such flows in regard to such flows in packed beds, ducts and pipes. However, very little experimental or theoretical research has been done on two-phase flow in pumps. Most notable of these are Pumps and Blowers--Two Phase Flow by A. J. Stepanoff (1)*, Air Handling Capability of Centrifugal Pumps by W. Biheller (2), Hydrodynamics of Flotation Cells by N. Arbiter, C. C. Harris, and R. F. Yap (3), and A Practical Three-Dimensional Flow Visualization Approach to the Complex Flow Characteristics in a Centrifugal Impeller by M. P. Boyce (4).

*The numbers in parenthesis refer to the list of references given on page 77.

ACKNOWLEDGEMENTS

The author is indebted to Dr. R.J. Raco, Dr.M. J. Levy, Professor R.M. Jacobs and Professor J.L. Polaner of Newark College of Engineering for their helpful advice, guidance and suggestions. He also wishes to thank the Worthington Corporation for donating the pump, W. Schmiedeskamp and his staff of Newark College of Engineering for their technical work on the apparatus, and R. Rabin and Jon Sinonian who read the manuscript a number of times.

TABLE OF CONTENTS

LIST OF TABLES

LIST OF FIGURES

CHAPTER I

INTRODUCTION

Statement of the Problem. The purpose of this study was to investigate the factors that limited the performance of the 1-inch long, open impeller centrifugal pump which was tested under air-water two phase flow conditions. Since there is an appreciable loss of discharge head with increased air flow rate, the study was aimed at determining the maximum possible air flow rate at each speed without sacrificing the developed head considerably.

This study attempts to define and explain unstable flow conditions caused by the accumulation of air at the impeller eye. In addition, discrepancies between this study and existing literature on the "breaking" of the head-capacity curve will be discussed. Finally, the effect of pump speed on the amount of air introduced will be investigated.

Importance and Limitations of the Study There has been a considerable amount of experimental and theoretical work performed on two phase flow in packed beds, ducts, and pipes, but very little research has been done on two phase flow in centrifugal pumps. The existing studies do not investigate

the pump flow parameters, namely the pump speed and water flow rate at which the air-handling capability of the pump is optimized. Moreover, these studies do not treat the pump speed as a variable parameter, whereas the effect of various pump speeds on the performance of the pump was one of the goals of this thesis.

Two phase flow in pumps has important industrial uses, in transporting mixtures of petroleum oil and natural gas. This case is one example where the separation of the gaseous and liquid phases at slower velocities complicates the estimation of the pipe frictional losses.

The results of this study were limited to the type of pump used. Comparison of the results of this study with those by Biheller[1] of the Worthington Corporation indicated that the design of the pump casing and the impeller vanes were the crucial factors for improving the air handling capability of the pump. This was evident in the maximum air-water volumetric ratio attained by Biheller (12%) as compared to a ratio of 6.8% achieved in this present study.

---

[1] W. Biheller, "Air Handling Capability of Centrifugal Pumps", Worthington Corporation Research Paper (Harrison, N.J., 1957)

Despite these limitations, this present study proved the usefulness of furthering the investigation of two-phase flow in pumps. While this present study clarified certain questions, it opened additional areas for further study. Detailed recommendations relative to structural changes in the apparatus (See figure 18) and a different experimental procedure are made in Chapter VI under summary.

A Preview Chapters II, III, and IV discuss the literary survey, the preliminary work on the apparatus, and the experimental procedure respectively. Chapter V, entitled "Discussion of Results", is given an extensive treatment. This chapter begins with a discussion of the factors that limit the performance of the centrifugal pump under two-phase flow conditions. One of these factors, the maximum possible air flow, is discussed in detail (See pages 17-20), and compared with Biheller's study. This is followed by a description of the unstable flow condition and how it is affected by the pump geometry (See page 20). A comparison of the pump performance curves is made between this study and Stepanoff's[2]. Following this, flow parameters are determined

[2] A.J. Stepanoff, Pumps and Blowers - Two Phase Flow, (New York: John Wiley and Sons, 1966) p.262

which optimize the air handling capability of the pump. Finally, chapter VI summarizes the findings of this present study and also recommends areas for further research and desired changes in the apparatus and the experimental procedure.

LIST OF NOTATION

a	Pump geometric constant
b	Pump geometric constant
β	Ratio of orifice throat diameter to inside pipe diameter
bhp	Brake horsepower
C	Coefficient of discharge
d	Orifice throat diameter, inch
D	Impeller diameter, inch
F	Velocity of approach factor
F_a	Factor accounting for thermal expansion of orifice
γ	Density of air-water mixture, lb_m/ft^3
g	Gravitational constant, $32.2 ft/sec^2$
H	Discharge pressure head, ft of water
h_L	Mechanical energy converted into heat, $ft\text{-}lb_f/lb_m$
h_{hg}	Pressure differential in manometer, in of mercury
h_w	" " " " in of water
L	Load on torque bar, lb_f
μ	Viscosity, $lb_f\text{-}sec/ft^2$
N	Number of impeller vanes
n	Pump efficiency
ω	Pump speed, rev/min

ω_c	Minimum pumping speed, rev/min
P	Pressure, lb_f/in^2
Q	Water flow rate, ft^3/sec
R	Universal Gas Constant, 53.35 $ft\text{-}lb_f/lb_m\text{-}^oR$
r	Lenght of torque arm, inch
ρ	Air density, lb_m/ft^3
T	Temperature of injected air, ^oR
V	Velocity, ft/sec
v	Specific volume, ft^3/lb_m
W	Energy added to fluid during pumping $ft\text{-}lb_f/lb_m$
w_h	Weight flow rate of air lb_m/hr
Y	Net expansion factor
z	Height, ft

CHAPTER II

Review of the Literature

Many analytical studies have been undertaken in two-phase flows. Most of these analyses are restricted to two-phase flows in pipes, ducts and packed beds, whereas very little research has been done on the air handling capability of centrifugal pumps. The limited studies available, analyse the means of improving the air handling capability of centrifugal pumps using such parameters as the geometry of the pump impeller and the casing, the suction pressure, and vane geometry. None of the studies investigates the air handling capability of centrifugal pumps under a variable pump speed. Consequently the question arises whether there is an optimal pump speed at which a maximum amount of air can be discharged without affecting the performance of the pump considerably.

The following is a brief summary of the existing experimental and theoretical work on two-phase flow in centrifugal pumps. Stepanoff[1], in investigating two-phase flow, concluded that "the ability of centrifugal pumps to

[1] A.J. Stepanoff, Pumps and Blowers--Two-Phase Flow John Wiley & Sons, Inc. New York, 1966, p.262

pump entrained gases is limited." He was able to attain an air-water volumetric ratio of 14% with a head-capacity curve that dropped with increasing air flow. In addition, the efficiency curve peaked at a lower capacity as the air-water volumetric ratio increased. He concluded that "the most important element controlling the volume of entrained gas is the suction pressure."[2] Stepanoff also stated that the breaking of the head-capacity curve, it is estimated, occurs when the volume of air equals to that of water.[3] Finally, according to Stepanoff, the importance of studying two-phase flow in centrifugal pumps is based upon its industrial uses in addition to its scientific value. He cited as an example the complications in estimating pipe friction losses when a mixture of natural gas and oil is flowing through pipe lines.

The Biheller study[4] involved primarily the improvement of air handling pump capability by using various impeller and pump casing configurations. Among the various changes tried were the impeller size, number of vanes, open or closed

---

[2] Ibid., loc. cit. pp. 262 - 272

[3] Ibid., p. 263

[4] W. Biheller, "Air Handling Capability of Centrifugal Pumps, Worthington Corporation Research Paper (Harrison, N.J. 1957)

impeller, suction and eye diameter, lenght of vanes and volute casing. An impeller with short, curved vanes enabled the pump to discharge an air-water mixture containing 12% air by volume. Moreover, there was close agreement between Stepanoff and Biheller in regard to the general shape of the pump performance curves. Biheller found that the short curved vane configuration of the impeller minimized the interference between the vanes and the air bubbles, thus facilitating their discharge. Among his other recommendations to improve the air handling characteristics of the pump were "a more circular volute", and "a circular shaped spiraled volute."

Arbiter, Harris and Yap[5], in studying the effects of aeration on the power requirements and solid suspension characteristics of floatation cells, briefly discussed two-phase flow in small centrifugal pumps. They derived an equation where water flow rate is a function of the air flow rate and certain pump design constants. Expressing their equation with the nomenclature of this study yields

$$Q = a(\omega - \omega_c)D^3 - \frac{bW_h}{3600\rho}$$

[5] N. Arbiter, C.C. Harris, and R.F. Yap "Hydrodynamics and Floatation Cells" Henry Krumb School of Mines, Columbia University, New York, Jan 1968, P.S.

Here a and b are pump geometric constants, ω_c is the minimum rotational speed for liquid flow, and D^3 is introduced for dimensional balance. This equation was not the result of any direct experimental investigation. It was based on the mass conservation equation and another equation expressing the total fluid as the sum of the air and water flows. Attempts to verify this equation by direct substitution of the result of the present study were unsuccessful. Arbiter et al did not verify this equation either, "no experiments were performed with scaled pumping equipment, so that the equation is not completely established"[8].

---

[8] Ibid. loc. cit.

CHAPTER III

Preliminary Work

The construction of the entire apparatus as shown in Figure 18, can be divided into three phases: the erection of the pipe network, the design and calibration of the flow meters, and finally some modifications to improve the performance of the total system.

Galvanized $1\frac{1}{4}$ inch steel pipe constituted the water pipeline while the air line was of 1-inch galvanized steel pipe. The water pipeline was an uncompressed, closed loop, feeding water to the pump from a 500-gallon tank and discharging it into the same reservoir(See figure 18).

Two flow meters were employed; a turbine meter, manufactured by the Potter Aeronautical Co. and commercially known as Pottermeter was used to measure the water flow rate, and an orifice was used to measure the air flow rate (See figure 21.). The turbine meter was calibrated by means of a stop watch, a weighing tank, and an electronic counter. Three groups of data were taken and a straight line calibration curve of electronic counts versus water flow rate in

in gallons per minute was obtained (See figure 16).

The ASME Power Test Code for flow meters measuring compressible fluids was used for calibrating the orifice. Certain geometric constants, e.g. inside diameter of pipe, orifice throat diameter, and an air reservoir pressure of 25 Psig were used to obtain this calibration curve. The calibration curve was derived from the calculations (See page 62) giving a plot of pounds of air per hour versus the pressure differential across the orifice where the pressure differential was measured by a mercury manometer (See figure 17).

During the first part of the experimentation, modifications in the form of additions and eliminations of certain components to the test apparatus(See figure 18) were found to be necessary. Water accumulated in the mercury manometer (See figure 21). This was attributed to water flowing back into the air line up to the vicinity of the orifice. Since the pressure taps across the orifice protruded from the lower part of the pipe, the water that accumulated flowed down through these taps and into the mercury manometer. To remedy the situation, these taps were made to protrude from the upper section of the air

line (See figure 21), and in addition, two traps were assembled and placed one on each side of the manometer (See figure 21). Thus the problem of water accumulation was eliminated.

A second turbine meter, initially installed on the discharge side of the pump some forty diameters away was intended to measure the combined air-water flow rate. It proved to be useless as it was inconsistent in measuring the mixed air-water flow. The inconsistencies were caused by air bubbles impacting the rotating blades of the meter. Consequently, the turbine meter installed in the low-pressure side of the pump was used to measure the water flow (See figure 18).

CHAPTER IV

Experimental Procedure

The test plan consisted of operating the pump at five different speeds: 1500, 2000, 2500, 3000, and 3500 RPM, the latter being the optimal speed of the pump at no-air flow conditions. At each speed air was injected into the suction pipe four inches before entering the impeller eye at the following volumetric flow rates: 1.4, 1.72, 2.18, and 2.65×10^{-3} ft^3/sec. The injection was made through a perforated 1/8-inch steel pipe with a conic piece of brass attached to its end to minimize turbulence (See Figure 20).

The experimental procedure consisted of a routine format. All possible combinations of the input variables pump speed, air flow rate and water flow rate were employed to determine their effect on the output parameters discharge pressure, suction pressure and torque. As the experiment progressed, the minimum possible air flow rate at a given pump speed and air flow became important. As the water flow rate was reduced further, the air-water volumetric ratio increased (air flow was constant while water flow

decreased), thus air became the predominate phase and the pump became air-bound (See Figures 1 to 5). This phenomenon is refered to as an unstable flow condition because the pump could no longer discharge the two phase mixture. The same phenomenon occured when the maximum possible air flow rate (2.65×10^{-3} $ft^3/sec.$) was exceeded. At this point of the experiment the air flow was shut off, allowing the pump to self-prime and new conditions were chosen. This unstable flow condition is discussed in detail in Chapter V.

CHAPTER V

Discussion of Results

There has been a paucity of research done in two-phase flow in centrifugal pumps. This chapter consolidates and extends the existing research. Furthermore, it discusses some limitations of the earlier investigations and clarifies perviously unexplained points.

During the experimental stage of the present investigation, it was noticed that two factors limited the performance of the centrifugal pump when it was tested under two phase flow conditions. The first limiting factor was the minimum value of the water flow rate just prior to unstable flow conditions. These flow conditions were characterized by a gradual and a continuous drop in the discharge pressure and the water flow rate, even though neither the air flow nor the water flow were varied. This unstable flow behavior can also be explained by the Bernoulli equation applied between inlet and outled of the pump:

$$\frac{V_1^2}{2} + \frac{P_1}{\gamma} + gz_1 - W = \frac{V_2^2}{2} + \frac{P_2}{\gamma} + gz_2 + h_L \quad \text{.....(i)*}$$

$$\text{or} \quad -W = \Delta\left(\frac{V^2}{2} + \frac{P}{\gamma} + gz\right) + h_L \quad \text{..... (ii)}$$

* Subscripts 1 and 2 refer to flow conditions upstream and downstream respectively relative, to be impeller eye.

The sum of the velocity and potential heads, upstream and downstream relative to the impeller eye, remained constant during the experiment. Equation (ii) was reduced to

$$-W \sim \Delta\left(\frac{P}{\gamma}\right) + h_{\ell} \quad \text{.....(iii)}$$

Here the density of the air-water mixture (γ) was decreasing because the volume of air in the mixture was increasing during the experiment. Thus because the density of the mixture was decreasing the actual discharge pressure developed in pumping it also decreased in order to balance equation (iii) until the pump became air-bound.

At this point, it is appropriate to discuss the reasons for the increased volume of air in the air-water mixture at the impeller eye. In this study, the long, mutually perpendicular structure (See figure 19) of the impeller vanes disturbed the helical flow pattern around the impeller (See figure 22) and thus prevented some of the injected air from being discharged. The air was trapped between the individual vanes, and the mixture was churned around inside the casing of the pump. In order to observe this phenomenon, a stroboscope and a Hycam motion picture camera were used separately. The stroboscope yielded a clearer view of a larger area than was possible with the Hycam camera.

The motion picture camera was used by M. P. Boyce in his study on three-dimensional flow visualization in a centrifugal impeller (4)*. Boyce injected a mixture of dibutyl phthalate globules and kerosene into the water stream, seeking to determine whether the globules would follow the streamlines. In order to accomplish this Boyce used the Fastax motion picture camera to photograph the globules as they passed through the impeller. In both studies, that is, Boyce's and the present investigation, the pump casing was replaced by a similarly machined plexiglass casing in order to make photographing possible. However the absence of a tripod was one reason why the results of the motion picture photography of the present study were not in clear focus, and thus it was decided to use the stroboscope for reasons already mentioned. With the use of the stroboscope, it was possible to view the mass of air trapped inside the casing forming a ring of bubbles whose radius varied from the hub to the outer tip of the impeller vanes (See Figure 23). It was noticed during the experiment that the radius of the ring of air bubbles varied directly with

---

* The number in parentheses indicates the reference given on page 77.

the rate of water flow. A qualitative representation of the relationship between the radius of the ring of air bubbles and the water flow rate is shown in Figure 17-A. This ring of bubbles was the main hinderance to the flow of water, and it eventually resulted in the drop of the water flow rate, the discharge head, and the suction head. The blockage offered by the ring of air bubbles to the flow of water was also a function of the rate of air accumulation in the impeller eye. This accumulation was the result of unstable flow conditions where the inflow of air into the impeller eye exceeded its outflow. This was attributed to the geometric factors mentioned above in addition to the suction pressure at the impeller eye which affected the volume of the air. Hence, a high negative (suction) pressure resulted in a high volume of air.

Therefore, in summary, the nature of the flow instability stimulated by the increasing volume of air at the impeller eye was the consequence of two factors. First, the impeller design prevented some of the air from leaving the impeller eye. Secondly, the high suction pressure caused air to occupy most of the volume at the impeller eye until the pump became air-bound. Further operation of the

pump under these conditions proved harmful to the shaft and the packing. This was due to the fact that the heat generated by friction was being absorbed by the pump shaft and the casing, while previously it was being dissipated by water circulation.

The second limiting factor was the maximum value of the air flow relative to the water flow rate at a constant pump speed before the unstable conditions set in. These unstable flow conditions were the result of the geometry of the impeller, the insufficient vacuum for self-priming due to the low density of air, and the incapability of the pump to discharge all of the injected air. The impact of these factors on the unstable flow conditions was discussed previously in explaining the decreasing density of the air-water mixture.

Because one of the objects of this thesis was to investigate the air handling capability of the pump, the second limiting factor, namely the maximum possible air flow will be considered in depth. Literature on the topic of air-water two-phase flow in centrifugal pumps is very limited. Two of the most relevent studies has been made by W. Biheller of the Advance Products Division of Worthington Corporation

and by A.J. Stepanoff. The results of Biheller's work (specifically those relative to the shape of the pump performance curves), basically agree with the results of the present study with a few exceptions. Both showed that the discharge head dropped as the water flow was reduced manually. This was in contrast to the no-air flow conditions where the head increased continuously as the water flow was reduced. In the present study as the water flow was reduced, the drop of the discharge head started at about 40 to 60 per cent of the pump capacity for an air-water volumetric ratio of 4.3 to 6.8 per cent (See figure 1-5). However, the Biheller study showed this drop initiated at a very low capacity, namely, about 20 per cent[1] of the pump capacity for an air-water volumetric ratio of 6 per cent.

Thus, there was a discrepency between Biheller's work and this present study in regard to the pump capacity at which a fixed ampunt of injected air resulted in the total loss of the discharge head. This can be explained by the fact that Biheller used an impeller with short, curved vanes. His impeller was able to pump air-water mixtures at lower

[1]W. Biheller, " Air Handling Capacity of Centrifugal Pumps" Worthington Corporation Research Paper, (Harrison, N.J., 1957), p.p.9

flow capacities than those achieved by the pump used in the present study because its vane configuration facilitated the discharge of air bubbles from the impeller eye. This would also explain the higher proportion of air in the air-water mixture achieved by Biheller as compared to the proportion of air attained in this present study.

Using the short, curved vane configuration, Biheller achieved an air-water volumetric ratio of 12 per cent, although this resulted in a considerable drop of the discharge head. On the other hand, the pump impeller in the present study had four long and straight vanes extending out radially (See figure 19), and the maximum air-water volumetric ratio attained was 6.8 per cent at a water flow rate of 15 GPM and a pump speed of 2500 RPM. This value (6.8%) was achieved just before the aforementioned unstable flow conditions took place. Similar ratios for pump speeds of 3000 and 3500 RPM at water flow rates of about 20 GPM were found to be 4.35 per cent and 4.9 per cent respectively.

Explaining the significance attributed to geometric factors, Biheller noted that the air-water mixture in the volute casing followed a hellical flow pattern.[2] This left

[2] Ibid. p.4

the air bubbles in the middle of the hellical stream preventing their return to the center of the impeller (See figure 23), and thus facilitating the discharge of these bubbles from the impeller eye. However, the factor that prevented this situation was the length of the impeller vanes of the pump tested as compared with the shorter, curved vanes of the impeller used by Biheller.

Another pertinent study of two-phase flow in centrifugal pumps was made by A.J. Stepanoff.[3] There was a close parallel between Stepanoff's findings and the results of this study except Stepanoff confined his investigation to only one pump speed (900 RPM). Both studies agreed on the shape of the head-capacity and the efficiency curves. Stepanoff's results concerning the flow capacity corresponding to the "the breaking of the head-capacity curve"[4] were also in close agreement with Biheller's. However, Stepanoff made no mention of the effect of the impeller vane geometry on the head-capacity curve.

---

[3] A.J. Stepanoff, Pumps and Blowers - Two-phase Flow. (New York: John Wiley and Sons, 1966), p.263

[4] Ibid. loc. cit.

Stepanoff also emphasized the importance of the net positive suction head (NPSH), in controlling the volume of the air at the impeller eye.[5] On the other hand, he made no mention of the accumulation of air at the impeller eye, a point that this author attributed to the pump geometry.

Stepanoff's use of only one pump speed (900 RPM) ignores the effect of pump speed on the air handling capability of the pump. Consequently pump speed, flow capacity and air flow rate were varied in the present study in search of the optimizing combination. Among the five different pump speeds, 2500 RPM seemed to be unique. Two features distinguished this speed from the rest. First, the head-capacity curves showed no uniformity at this speed (See figure 3) while the corresponding curves at the other speeds were characterized by a clear symmetry around 20 GPM(See figure 1,2,4,5.) Secondly, at pump speeds of 3500 and 3000 RPM, the appreciable loss of the discharge head upon reduction of the water flow rate started at an air flow rate of 2.18×10^{-3} ft^3/sec (See figures 1 and 2) while the corresponding figure at 2000 and 1500 RPM was 1.72×10^{-3} ft^3/sec (See figures 4 and 5).

---

[5] Ibid. loc. cit.

However, at a pump speed of 2500 RPM, it was possible to increase the air flow rate up to 2.34×10^{-3} ft^3/sec (See figure 3) without an appreciable deviation of the head-capacity curve from its no-air behavior. Therefore, at 2500 RPM the pump was able to handle more air than at other speeds without a considerable loss of its discharge head. Also at this speed and air flow, the corresponding pump efficiency was not considerably different from its value at no air flow conditions. All of these observations led the author to believe that for this specific pump, optimal air handling conditions occured at a pump speed of 2500 RPM, a water flow rate of 15 GPM, and an air flow rate of 2.34×10^{-3} ft^3/sec. The optimal flow conditions at no-air flow, according to the experimental results as well as the manufacturer's data, were at 3550 RPM and a water flow rate of 35 GPM. Thus, the optimal values of the water flow and the pump speed were markedly reduced by the injection of air into the water stream. The mentioned optimal two-phase flow parameters, namely pump speed, capacity and air flow were obtained by trying various pump speeds as previously discussed. However, speed was not a variable in either Biheller's or Stepanoff's study as they investigated two-phase flow at only one pump speed. Thus it was impossible to make any conclusions from their

studies in regard to the effect of pump speed on the optimal air handling capability of their pumps.

Finally, one observation was made relative to the head-capacity and the efficiency curves. At the higher air flow rates, the peaks of the head-capacity and the efficiency curves coincided at the same pump flow capacity and speed. The explanation for this is that at the pump flow capacity when the air flow rate just exceeded the maximum amount that the pump could handle, the discharge head and the water flow rate decreased continuously for reasons discussed earlier in this chapter (See page 18). With the aid of the pump efficiency equation,

$$\eta = \frac{Q\gamma H}{550\ bhp}$$

it is clearly seen that simultaneous drops in Q and H will result in a similar drop of the efficiency.

The efficiency curves were clearly affected also by the increase of air in the air-water mixture. This resulted in a shift in the efficiency curves such that they peaked at a lower efficiency value and at a lower flow capacity(a result also achieved by Stepanoff)[6]. This behavior can also be explained by the simultaneous drop in the discharge head and the water flow rate.

[6] Ibid. p.262

CHAPTER VI

Summary and Recommendations

This study investigated the effects of two phase flow on the performance of the centrifugal pump tested. Some of the results compared favorably with existing literature while a comparison of other results was impossible due to limited published work on the topic of two phase flow in centrifugal pumps.

Two phase flow was found to affect the efficiency of the centrifugal pump tested. Increasing the flow capacity under no-air flow conditions resulted in a continuous drop of the discharge head, but upon introduction of an air flow greater than 1.72×10^{-3} $ft^3/sec.$, the discharge head increased up to a limit before it dropped to zero (See figures 1 to 5). It was found that increasing the air injection rate had an adverse effect on the performance of the pump in terms of total head.

Two factors are noted in explaining the behavior of the head-capacity curves: First, the geometry of the impeller vanes and the casing and, secondly, the suction pressure at the impeller eye. It was observed that the length of the

the impeller vanes (See Figure 19) interfered with the discharge of some of the air bubbles. These bubbles were trapped between the vanes. The high suction pressure at the impeller eye increased the volume of these bubbles such that they formed a partial block to the incoming flow. It was concluded that the mass of air inside the casing increased with time until it completely blocked the flow.

Another finding of this study was the determination of the values of the flow parameters, pump speed and flow capacity which resulted in optimal two-phase flow conditions. It was concluded that with the introduction of air into the water stream, the pump speed at which maximum air was discharged without a considerable head loss was below its optimal speed at no-air flow. Optimal two-phase flow conditions were observed at a pump speed of 2500 RPM and a flow capacity of 15 GPM. Optimal no-air flow conditions were observed at 3550 RPM and 35 GPM.

Recommendations: The remainder of this chapter is devoted to the discussion of recommended areas for further study, and and desired structural and procedural changes in the experiment. While clarifying certain aspects of two-phase flow in

pumps, this study introduced new areas for further investigation. One of these areas involves the effects of varying the pump speed at fixed air and water flow rates on the developed discharge head. This may shed some light on the problem of phase separation at slower flow velocities as well as the air accumulation inside the pump casing.

It is recommended that the experimental procedure of this study be repeated using the following pump configurations:

1.- A 7-inch impeller with curved vanes in conjunction with the existing plexiglass casing.

2.- A 5-inch impeller with curved vanes also with the present casing.

3.- A 7-inch impeller with curved vanes with a wider volute casing.

4.- A 5-inch impeller with curved vanes with a wider volute casing.

It is also recommended that with each of these four pump configurations an experimental procedure be followed whereby the pump speed is varied at fixed air and water flow rates, while the discharge and suction heads are measured.

From a structural viewpoint, the apparatus can be considerably improved. First, a valve should be installed on the suction side of the pump to stop the water from flowing from the elevated reservoir to the pump during repairs. Secondly, it is advisable to resort to an alternative source of compressed air as oil (traceable to the compressor) was detected in the reservoir. Of course this contamination can be prevented by the use of filters and separators, however the alternate source of compressed air already mentioned is conveniently located. Thirdly, the reservoir should be permanently covered to keep solid particles out of the system. Fourthly, in order to increase the suction pressure it is recommended that the water reservoir be placed a few floors above the laboratory. The final recommendation is to improve the means of measurement and control of the air flow. The existing orifice-manometer combination does not constitute an accurate air flow measuring system, because of the excessive joints and fittings in its construction (See figure 21). A method of improving this situation would be to install a compact air flow meter and a needle valve in the air line in order to obtain a finer control of the air flow rate.

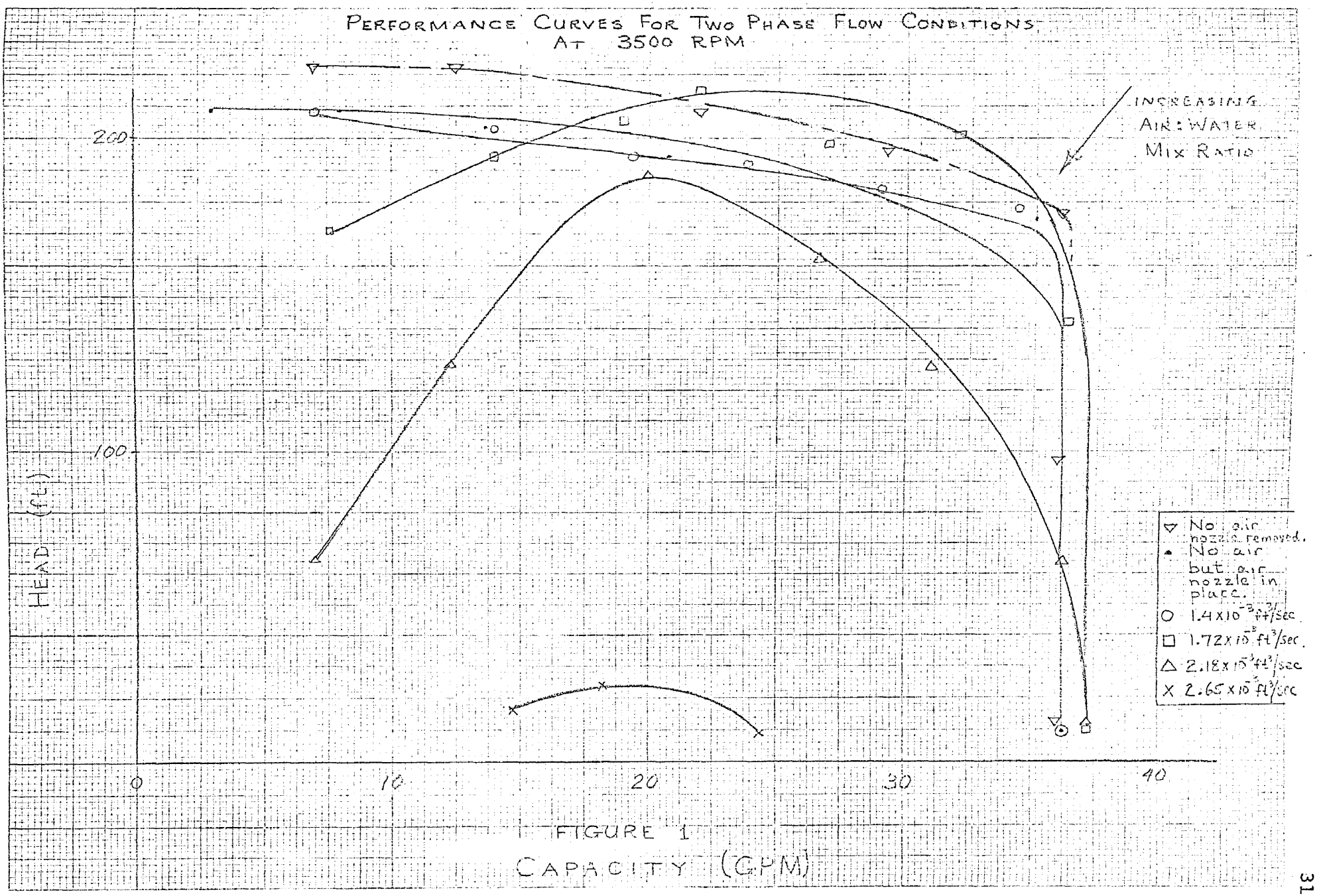
PERFORMANCE CURVES FOR TWO PHASE FLOW CONDITIONS
AT 3500 RPM
INCREASING
AIR : WATER
MIX RATIO
HEAD (ft.)
200
100
0
10
20
30
40
CAPACITY (GPM)
No air nozzle removed.
No air but air nozzle in place.
1.4 x 10⁻³ ft³/sec
1.72 x 10⁻³ ft³/sec
2.18 x 10⁻³ ft³/sec
2.65 x 10⁻³ ft³/sec

FIGURE 1

PERFORMANCE CURVES FOR TWO PHASE FLOW CONDITIONS AT 3000 RPM

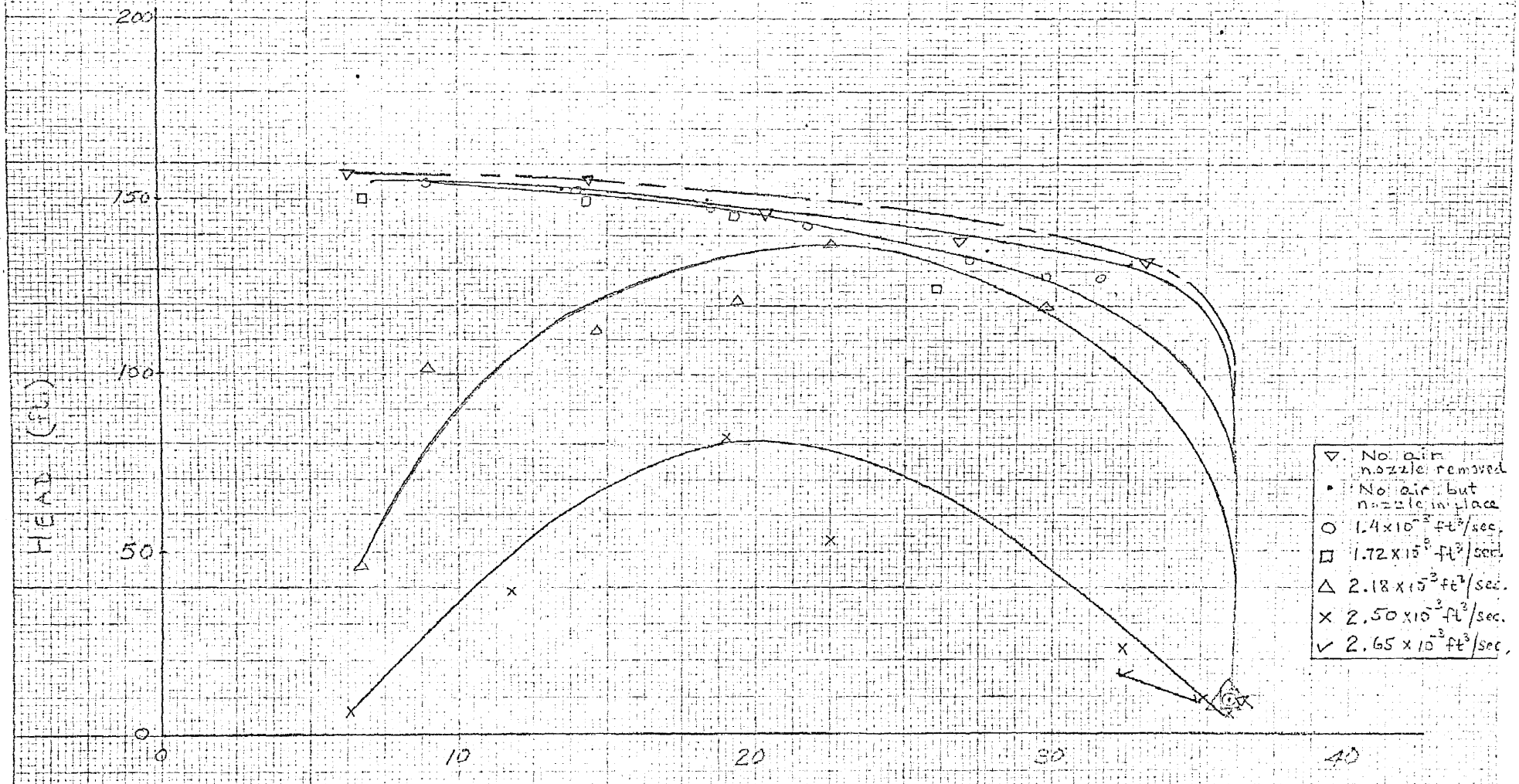

FIGURE 2

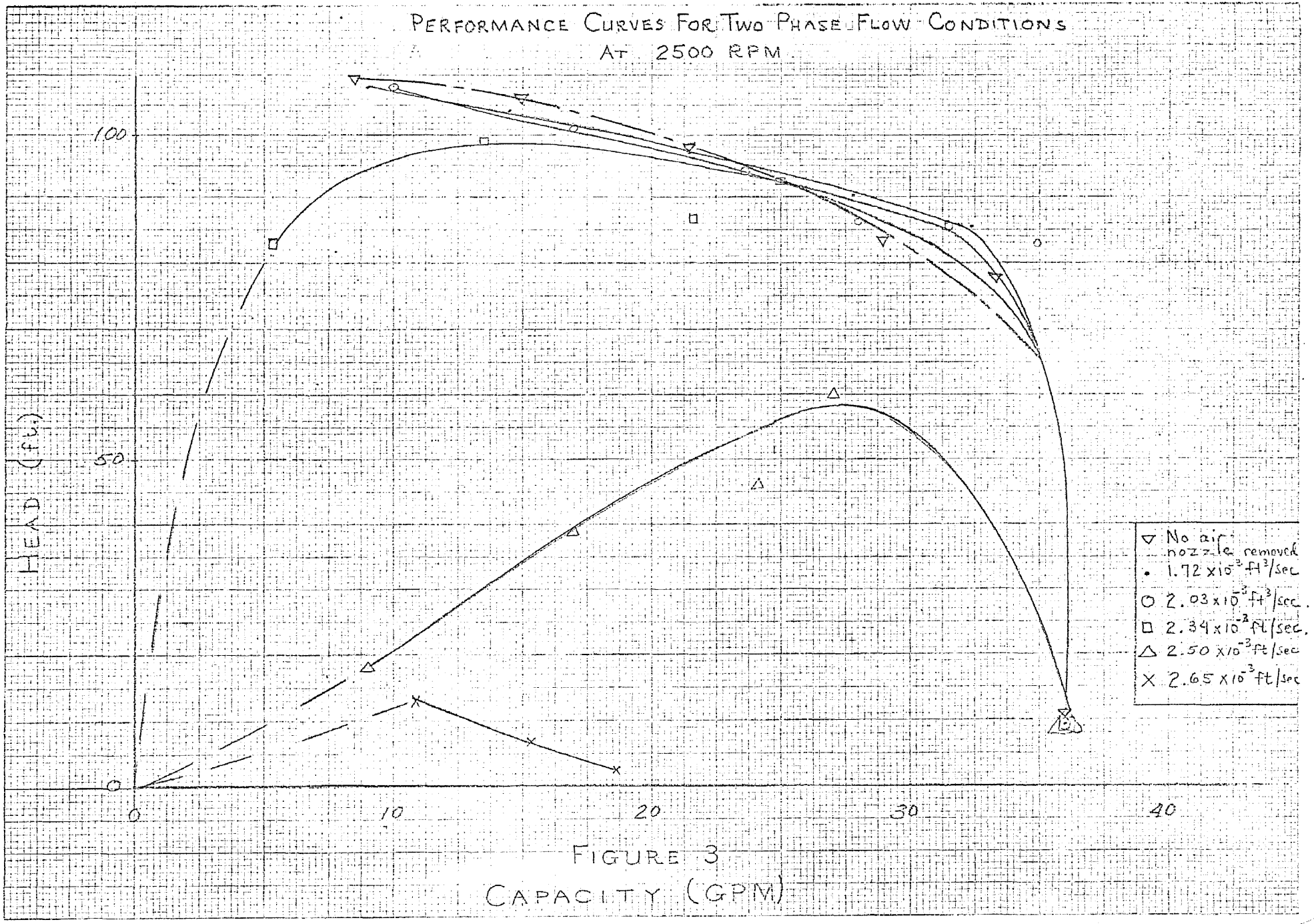
PERFORMANCE CURVES FOR TWO PHASE FLOW CONDITIONS
AT 2500 RPM
HEAD (ft.)
100
50
0
0
10
20
30
40
CAPACITY (GPM)
▽ No air nozzle removed
• 1.72 x 10⁻³ ft³/sec
○ 2.03 x 10⁻³ ft³/sec.
□ 2.34 x 10⁻³ ft/sec.
△ 2.50 x 10⁻³ ft/sec
× 2.65 x 10⁻³ ft/sec

FIGURE 3

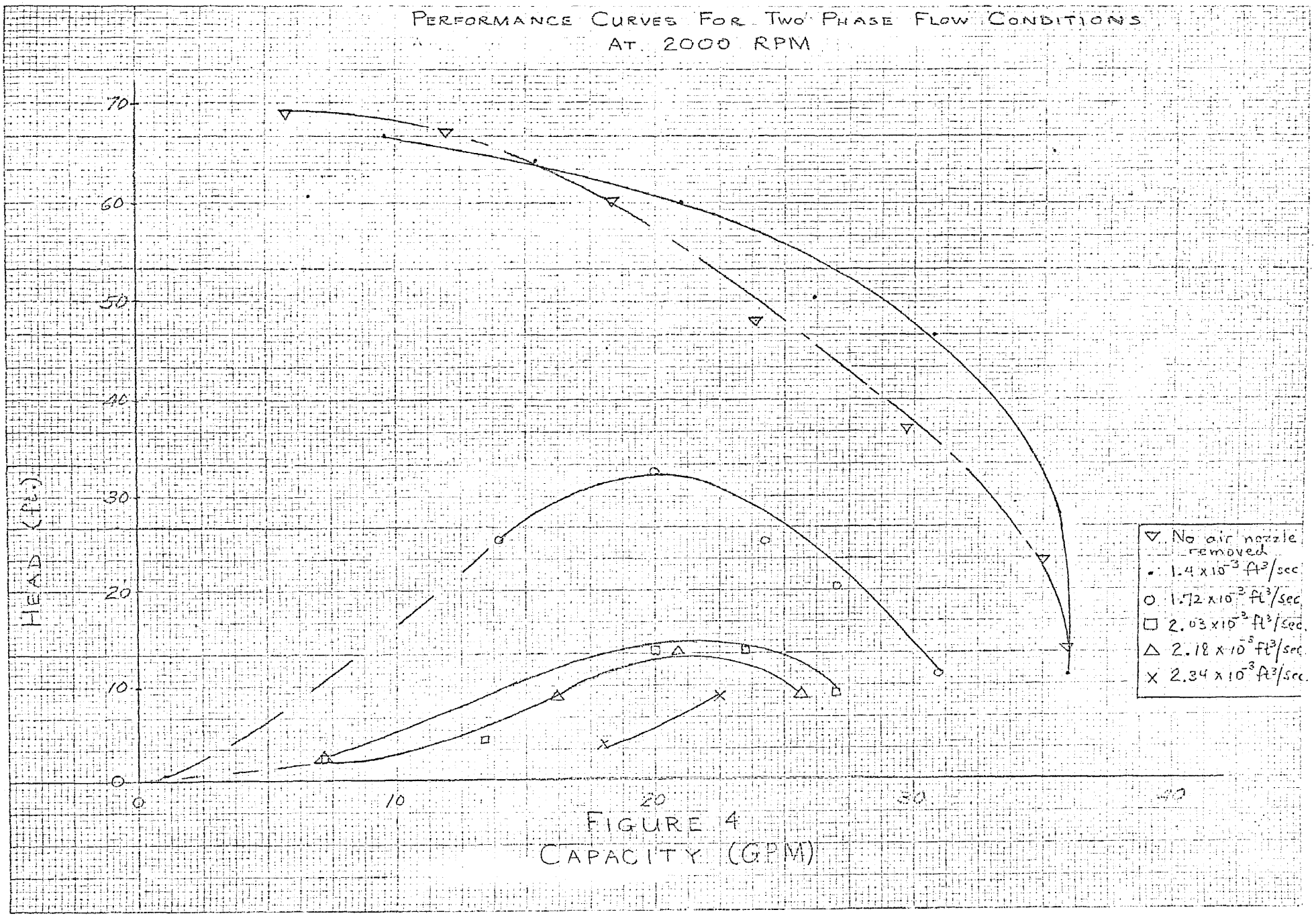
PERFORMANCE CURVES FOR TWO PHASE FLOW CONDITIONS
AT 2000 RPM
70
60
50
40
30
20
10
0
H_{wA} (ft.)
0
10
20
30
40
CAPACITY (GPM)
No air nozzle removed
1.4×10^{-3} ft³/sec
1.72×10^{-3} ft³/sec
2.03×10^{-3} ft³/sec
2.18×10^{-3} ft³/sec
2.34×10^{-3} ft³/sec

FIGURE 4

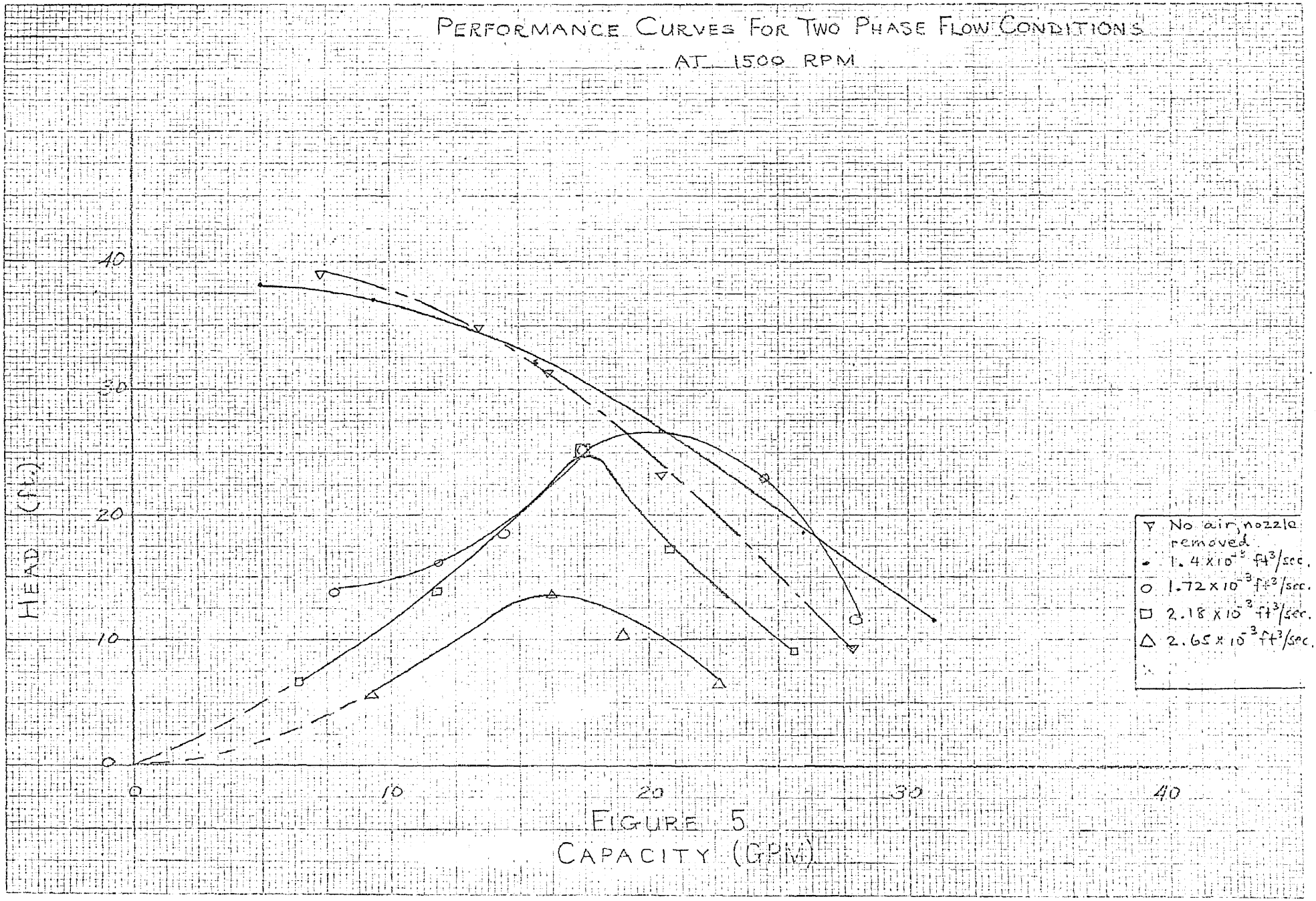
PERFORMANCE CURVES FOR TWO PHASE FLOW CONDITIONS
AT 1500 RPM
HEAD (FT.)
CAPACITY (GPM)
0
10
20
30
40
No air, nozzle removed
1.4 x 10⁻³ ft³/sec.
1.72 x 10⁻³ ft³/sec.
2.18 x 10⁻³ ft³/sec.
2.65 x 10⁻³ ft³/sec.

FIGURE 5

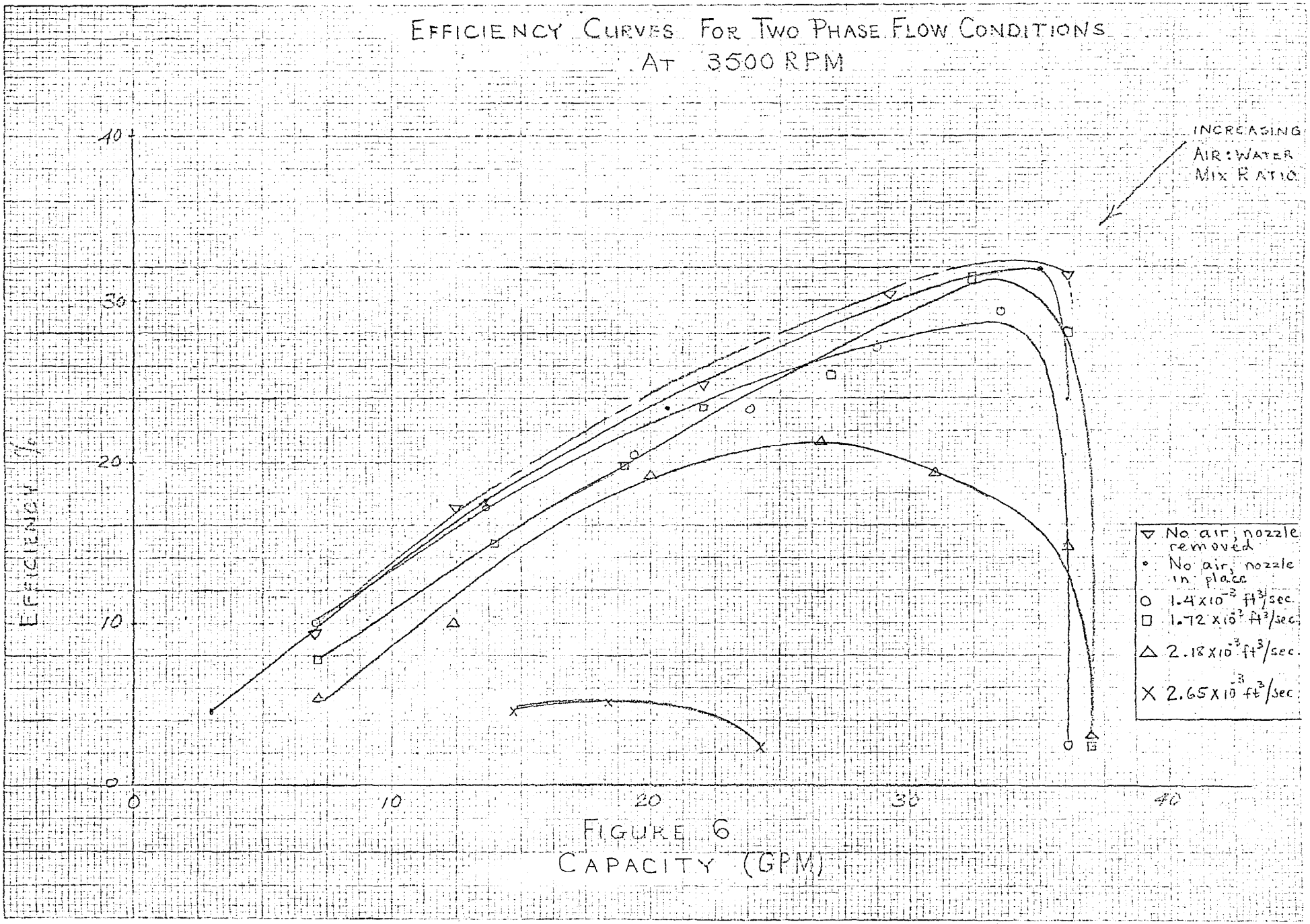
EFFICIENCY CURVES FOR TWO PHASE FLOW CONDITIONS
AT 3500 RPM
INCREASING
AIR : WATER
MIX RATIO
EFFICIENCY %
0
10
20
30
40
No air, nozzle removed
No air, nozzle in place
1.4 x 10⁻³ ft³/sec.
1.72 x 10⁻³ ft³/sec.
2.18 x 10⁻³ ft³/sec.
2.65 x 10⁻³ ft³/sec.
CAPACITY (GPM)

FIGURE 6

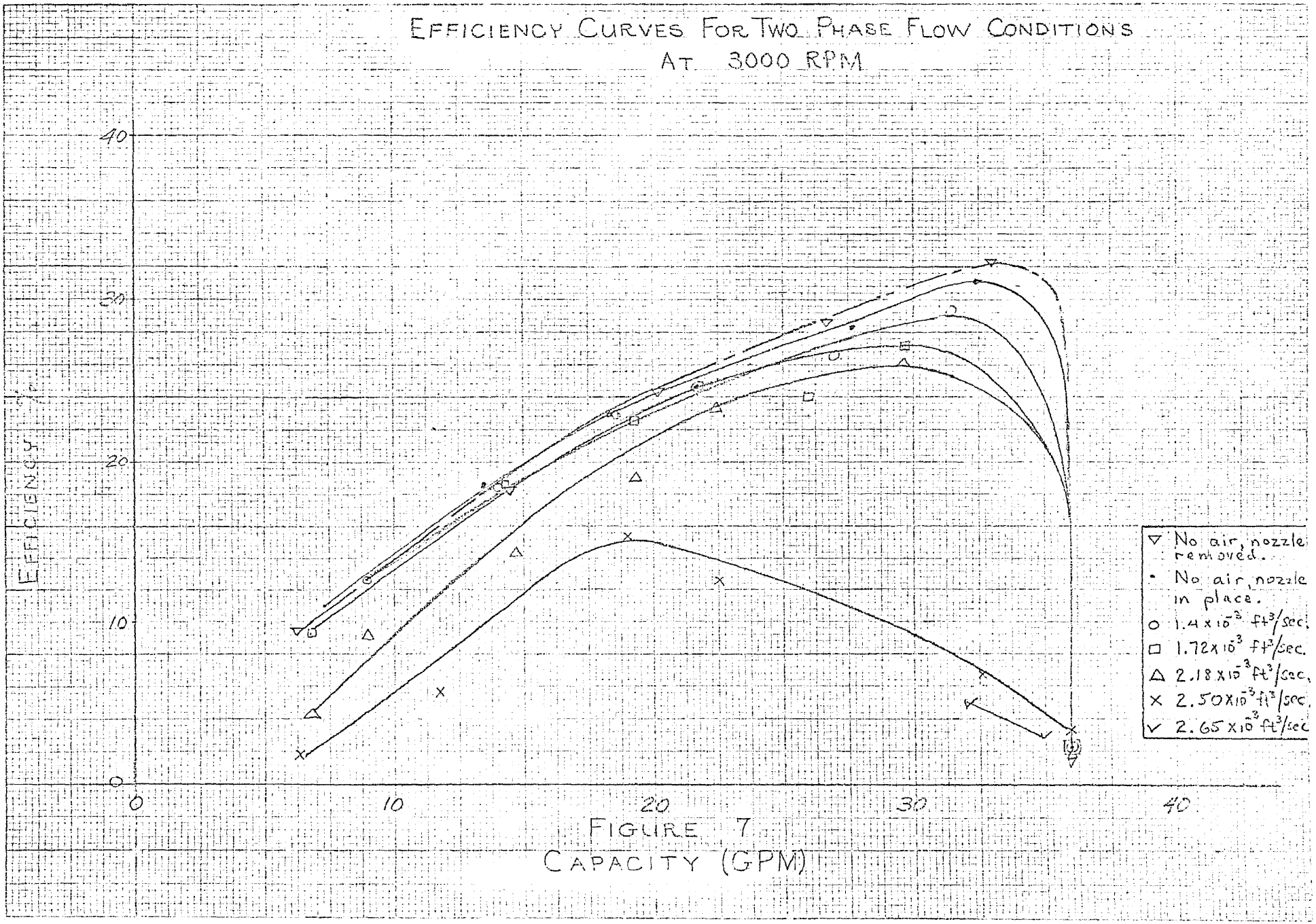
EFFICIENCY CURVES FOR TWO PHASE FLOW CONDITIONS
AT 3000 RPM
EFFICIENCY
40
30
20
10
0
0
10
20
30
40
CAPACITY (GPM)
▽ No air, nozzle removed.
• No air, nozzle in place.
○ 1.4 x 10⁻³ ft³/sec.
□ 1.72 x 10⁻³ ft³/sec.
△ 2.18 x 10⁻³ ft³/sec.
× 2.50 x 10⁻³ ft³/sec.
✓ 2.65 x 10⁻³ ft³/sec

FIGURE 7

Efficiency Curves For Two Phase Flow Conditions At 2500 RPM

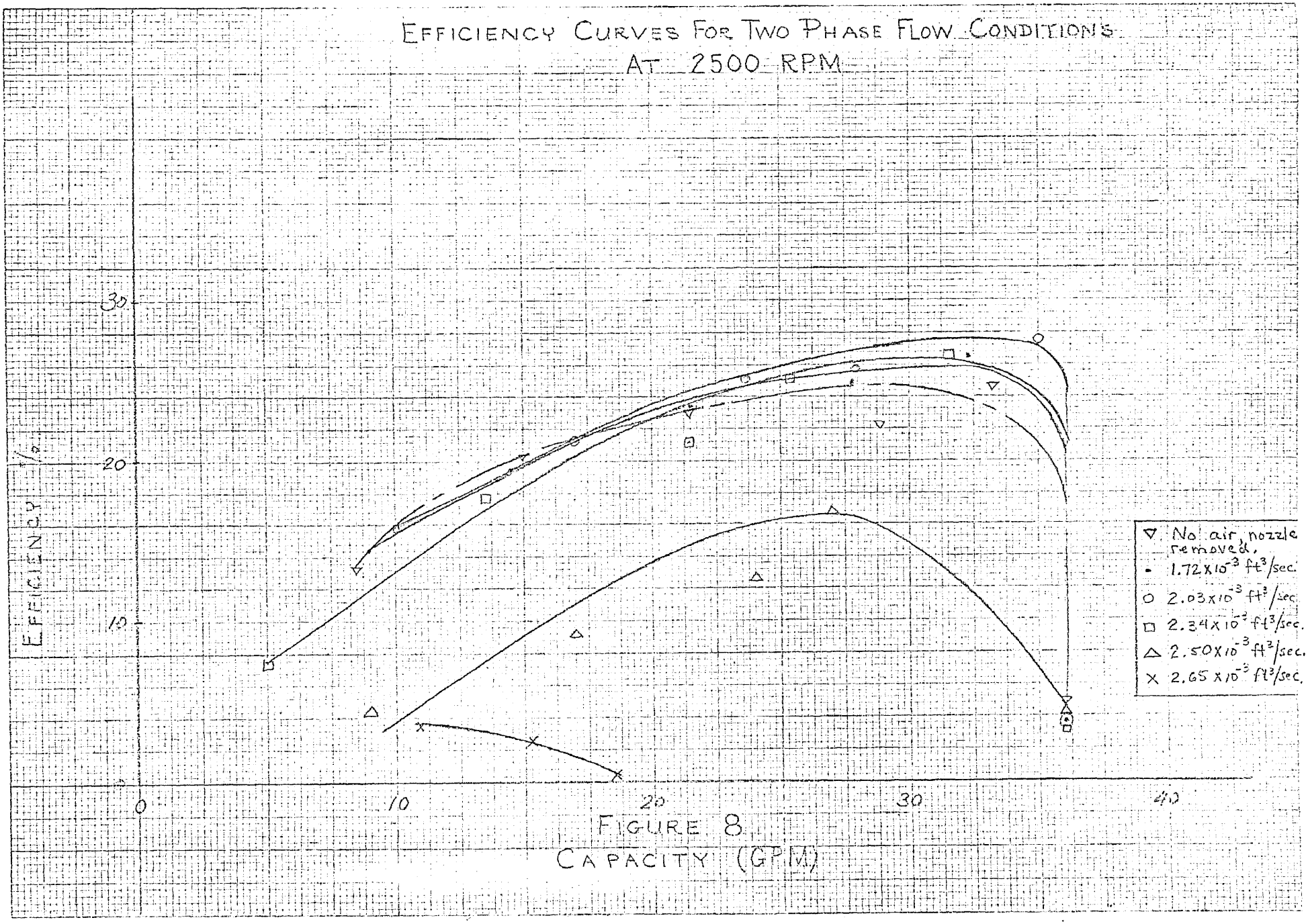

Figure 8

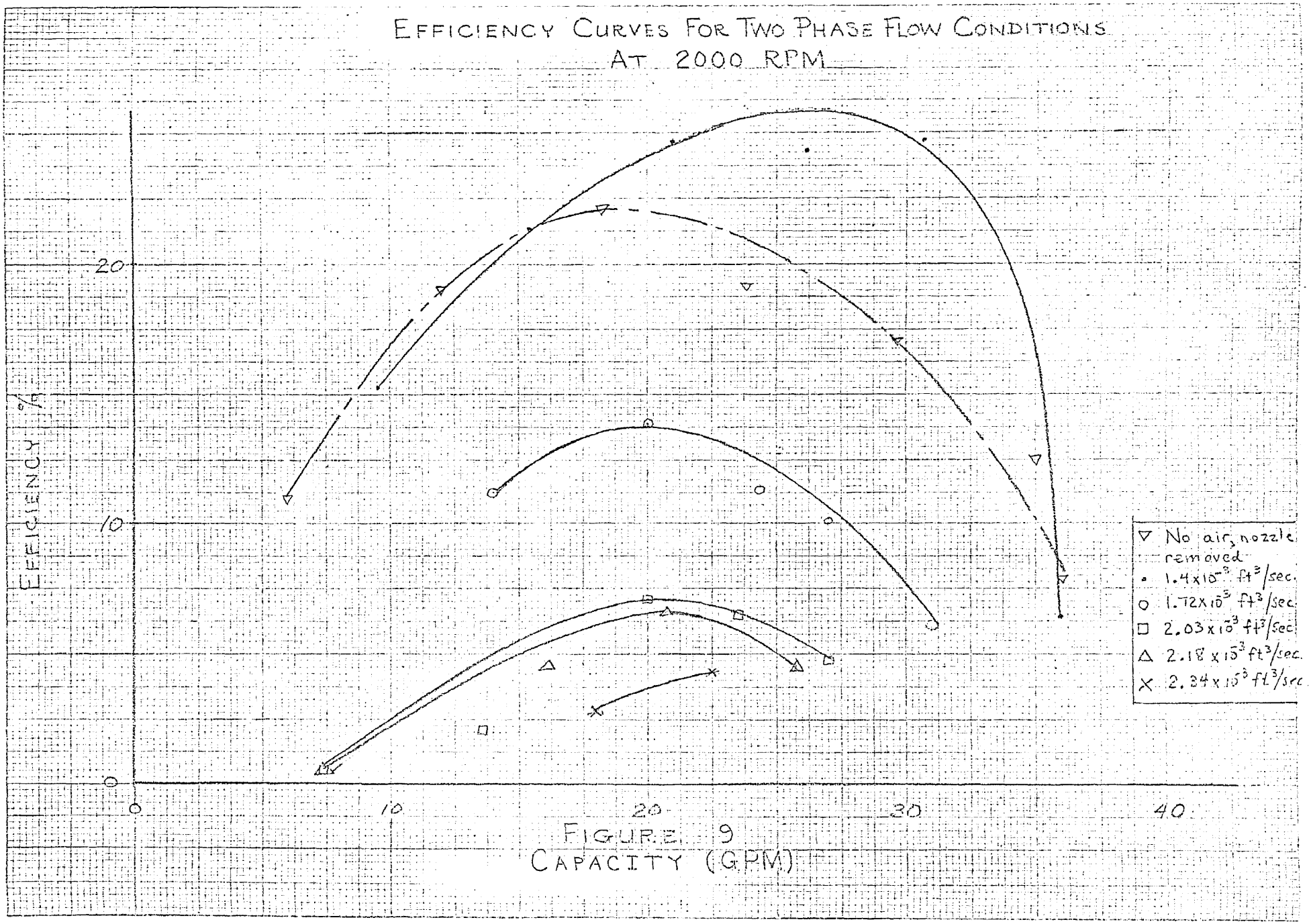
EFFICIENCY CURVES FOR TWO PHASE FLOW CONDITIONS
AT 2000 RPM
EFFICIENCY %
20
10
10
20
30
40
CAPACITY (GPM)
No air, nozzle removed
1.4x10⁻³ ft³/sec.
1.72x10⁻³ ft³/sec.
2.03x10⁻³ ft³/sec.
2.18 x 10⁻³ ft³/sec.
2.34 x 10⁻³ ft³/sec

FIGURE 9

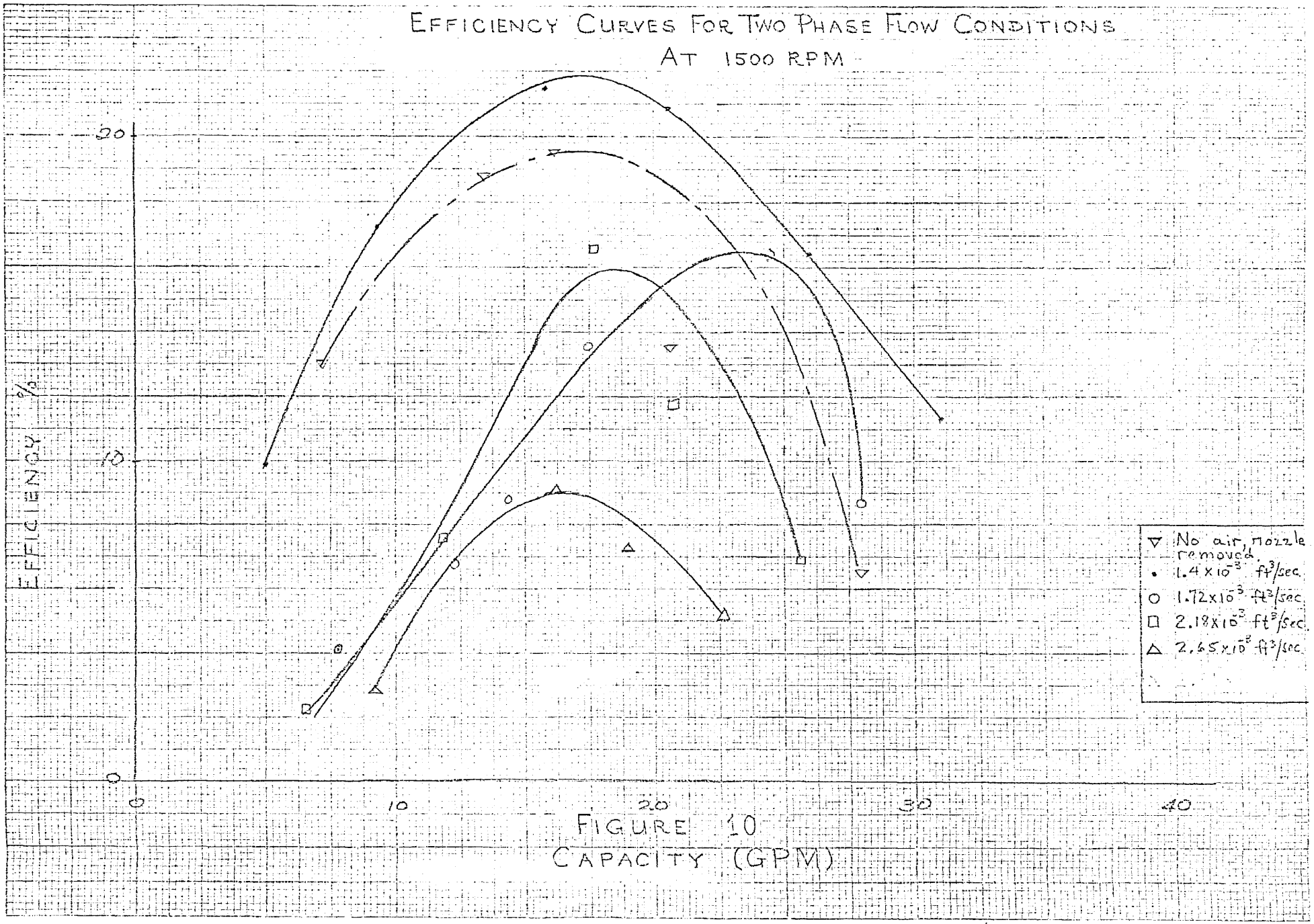
EFFICIENCY CURVES FOR TWO PHASE FLOW CONDITIONS
AT 1500 RPM
EFFICIENCY %
20
10
0
0
10
20
30
40
CAPACITY (GPM)
No air, nozzle removed.
1.4 x 10⁻³ ft³/sec.
1.72 x 10⁻³ ft³/sec.
2.18 x 10⁻³ ft³/sec.
2.65 x 10⁻³ ft³/sec.

FIGURE 10

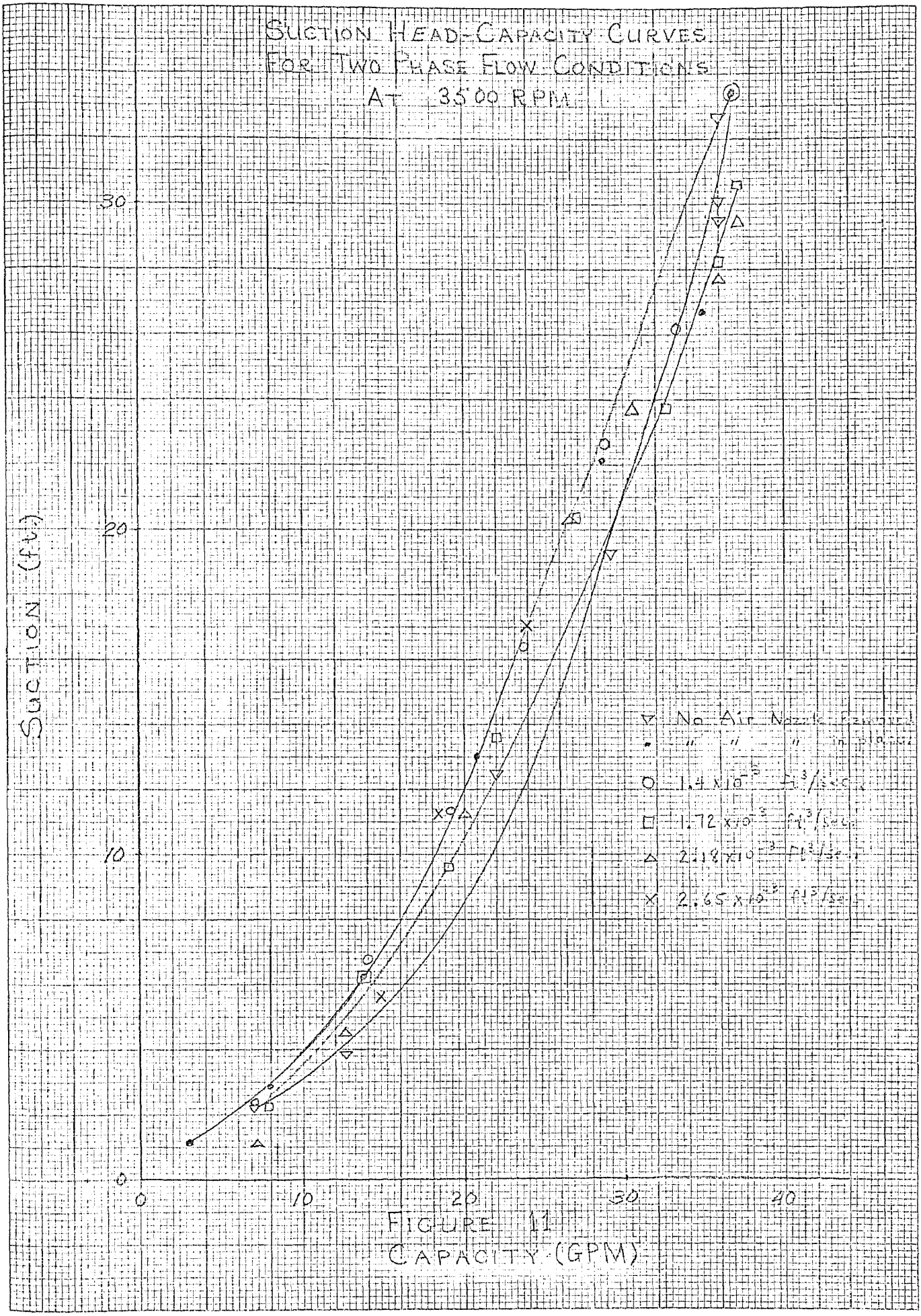
SUCTION HEAD-CAPACITY CURVES
FOR TWO PHASE FLOW CONDITIONS
AT 3500 RPM
SUCTION (ft.)
CAPACITY (GPM)
0
10
20
30
40
No Air Nozzle Flow
" " " in
1.4 x 10⁻³ ft³/sec
1.72 x 10⁻³ ft³/sec
2.18 x 10⁻³ ft³/sec
2.65 x 10⁻³ ft³/sec

FIGURE 11

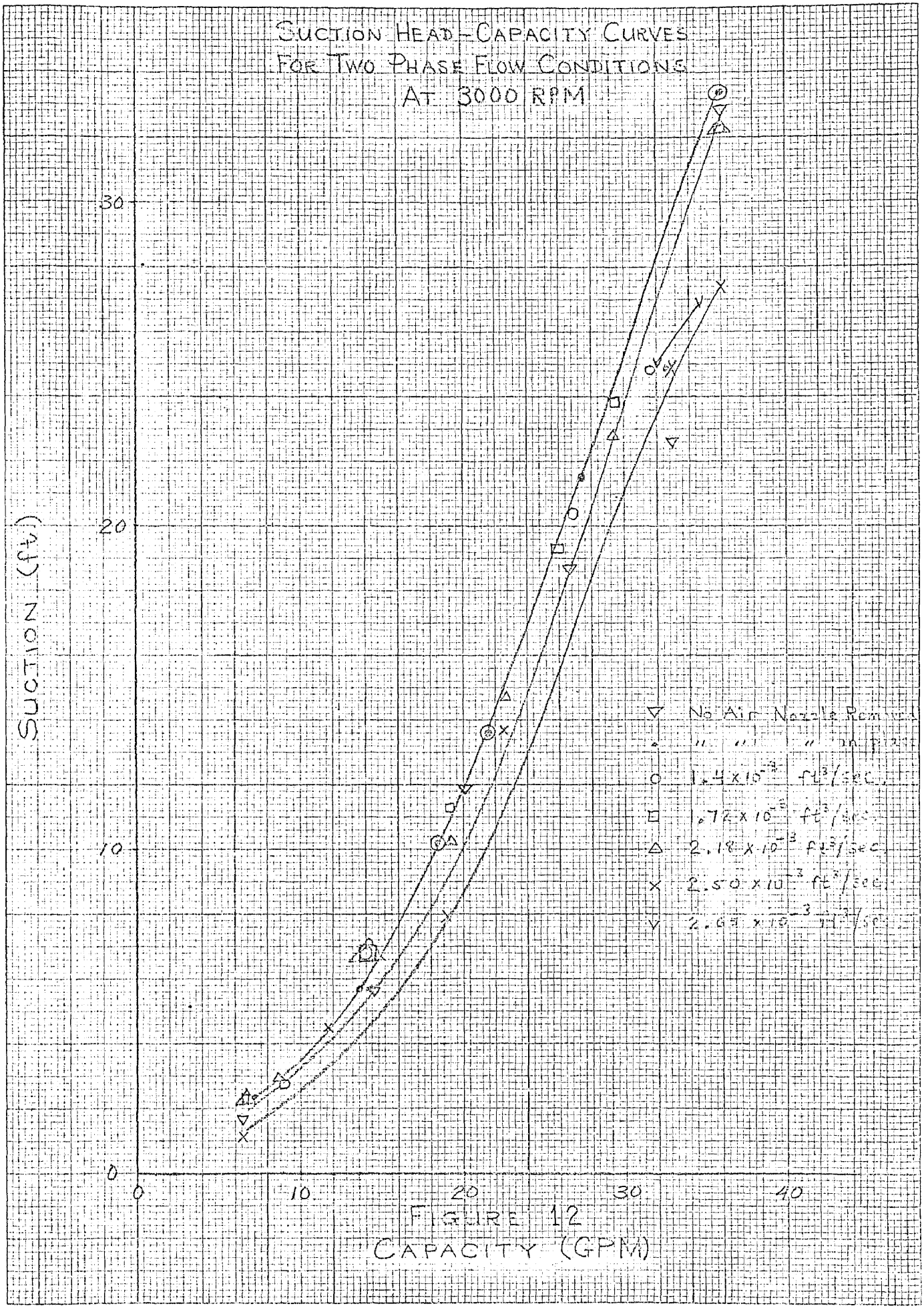
SUCTION HEAD – CAPACITY CURVES
FOR TWO PHASE FLOW CONDITIONS
AT 3000 RPM
SUCTION (ft.)
CAPACITY (GPM)
0
10
20
30
40
No Air Nozzle Removed
1.72 x 10⁻³ ft³/sec
2.18 x 10⁻³ ft³/sec
2.50 x 10⁻³ ft³/sec

FIGURE 12

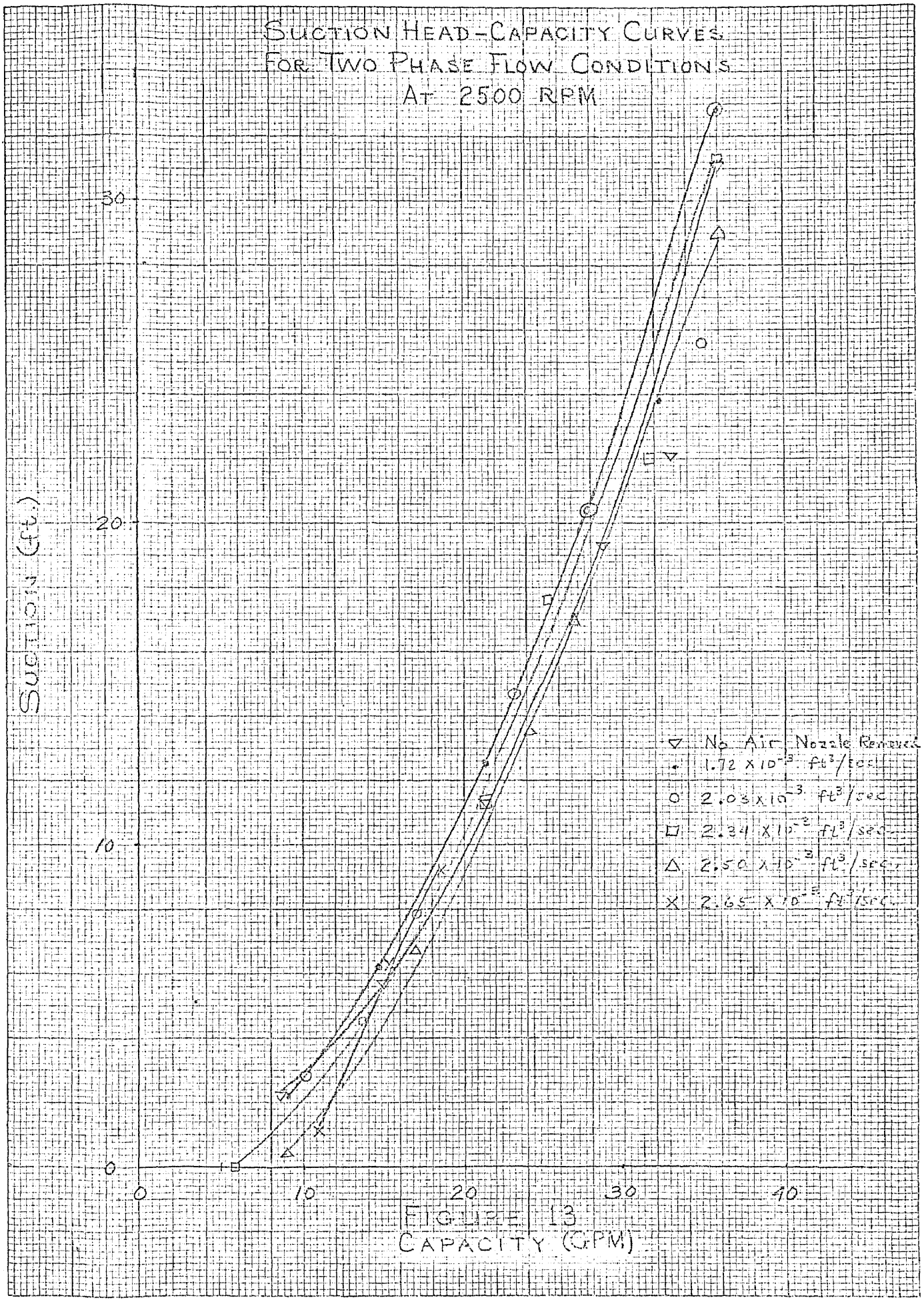
SUCTION HEAD-CAPACITY CURVES
FOR TWO PHASE FLOW CONDITIONS
AT 2500 RPM
SUCTION (ft.)
CAPACITY (GPM)
30
20
10
0
0
10
20
30
40
No Air Nozzle Removed
1.72 X 10⁻³ ft³/sec
2.03 X 10⁻³ ft³/sec
2.34 X 10⁻³ ft³/sec
2.50 X 10⁻³ ft³/sec
2.65 X 10⁻³ ft³/sec

FIGURE 13

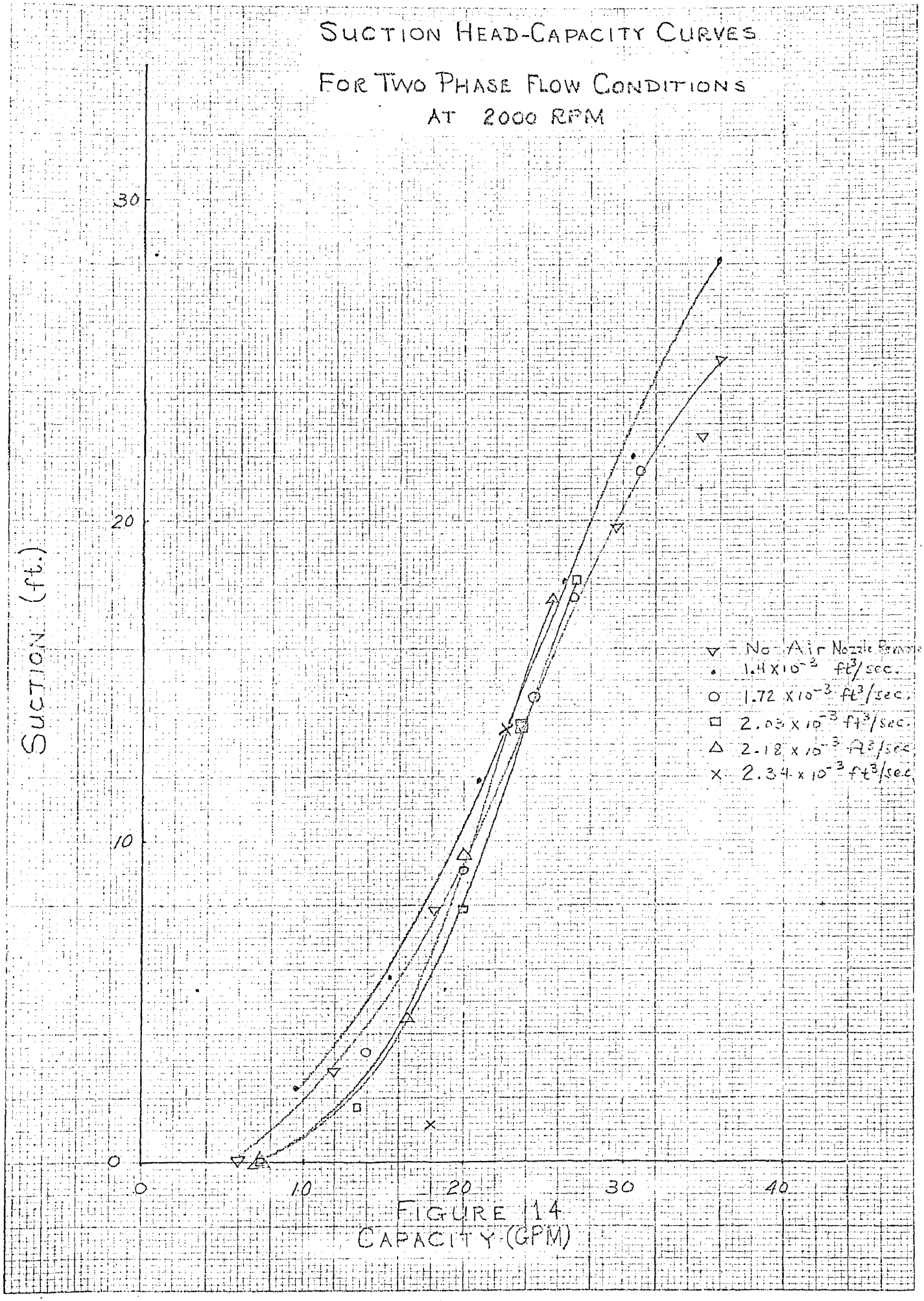
SUCTION HEAD-CAPACITY CURVES
FOR TWO PHASE FLOW CONDITIONS
AT 2000 RPM
SUCTION (ft.)
30
20
10
0
0
10
20
30
40
CAPACITY (GPM)
▽ - No Air Nozzle Pressure
• 1.4 x 10⁻³ ft³/sec.
○ 1.72 x 10⁻³ ft³/sec.
□ 2.03 x 10⁻³ ft³/sec.
△ 2.18 x 10⁻³ ft³/sec.
× 2.34 x 10⁻³ ft³/sec.

FIGURE 14

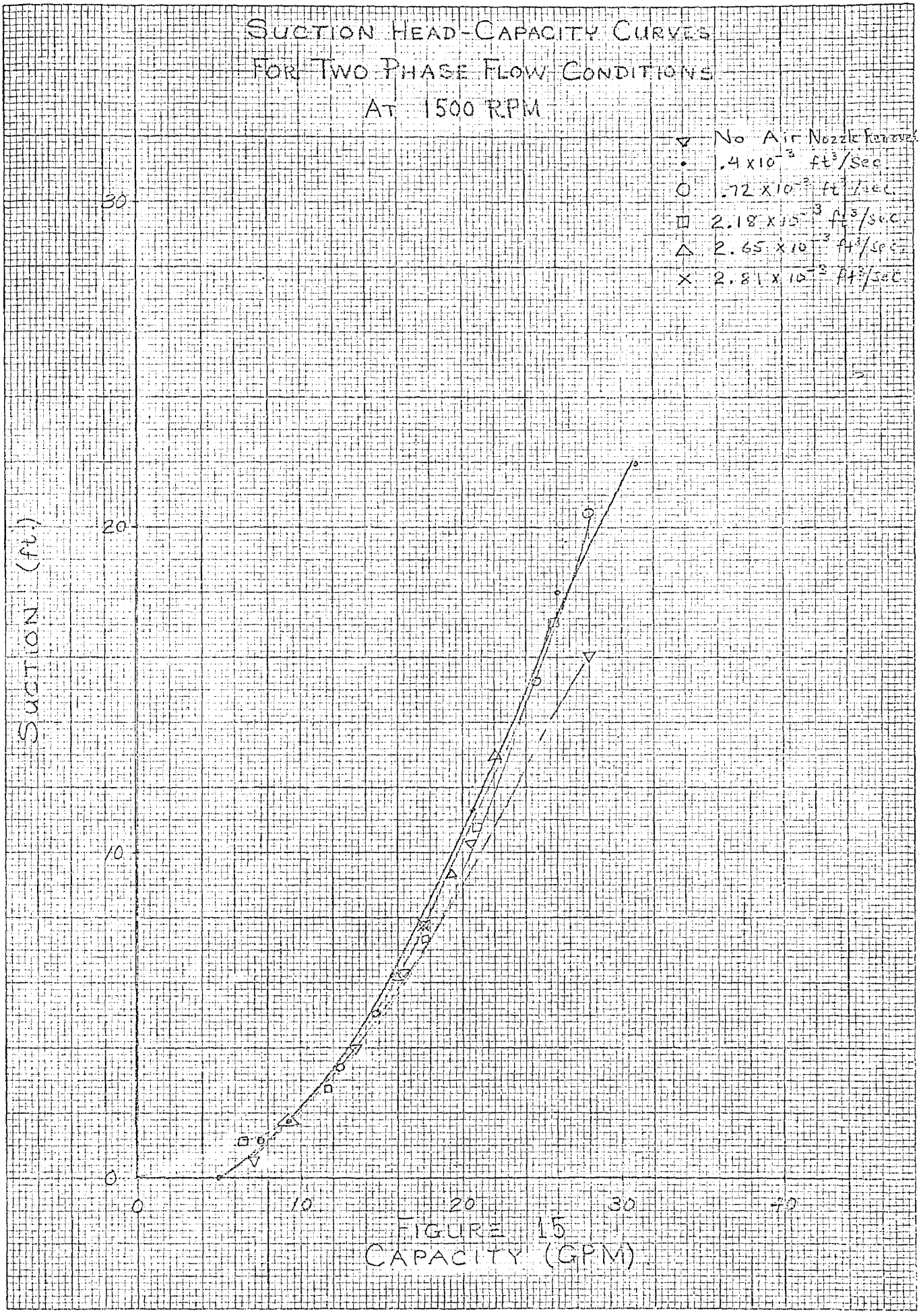
SUCTION HEAD-CAPACITY CURVES
FOR TWO PHASE FLOW CONDITIONS
AT 1500 RPM
No Air Nozzle Removed
1.4 x 10⁻³ ft³/Sec.
1.72 x 10⁻³ ft³/Sec.
2.18 x 10⁻³ ft³/Sec.
2.65 x 10⁻³ ft³/Sec.
2.81 x 10⁻³ ft³/Sec.
SUCTION (ft.)
0
10
20
30
0
10
20
30
40
CAPACITY (GPM)

FIGURE 15

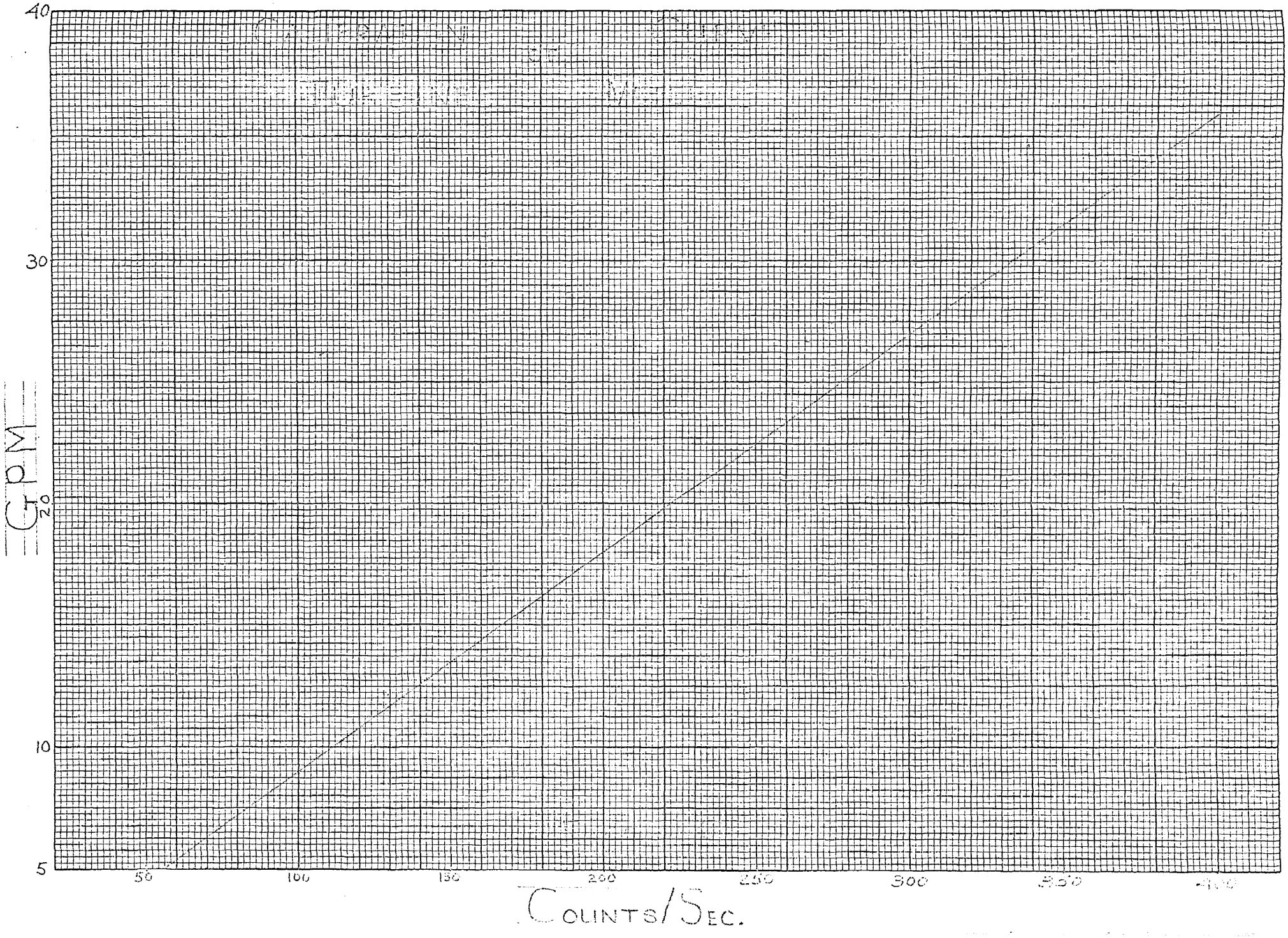
40
30
20
10
5
CPM
50
100
150
200
250
300
350
400
COUNTS/SEC.

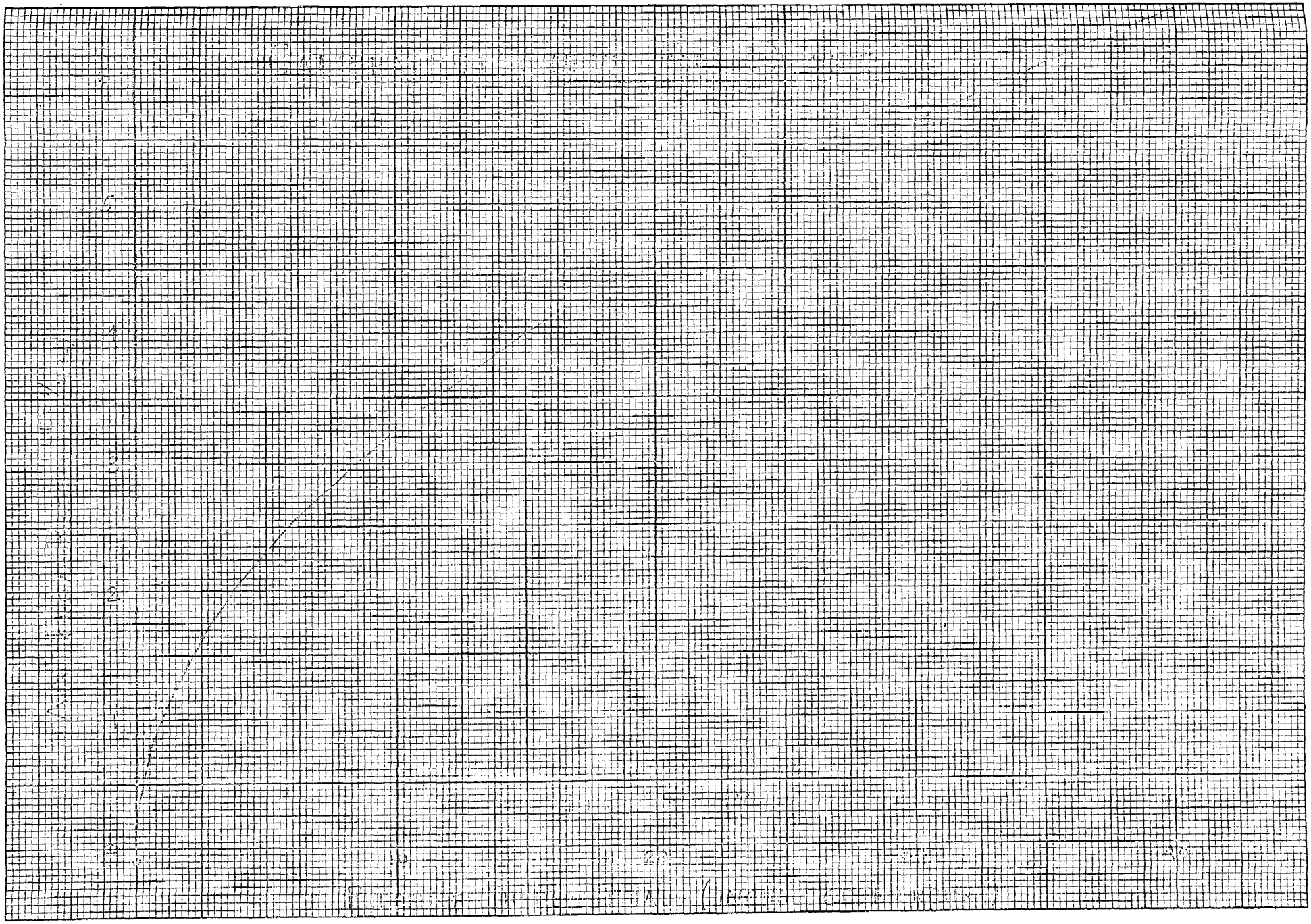

A QUALITATIVE RELATIONSHIP BETWEEN RADIUS OF RING OF AIR BUBBLES INSIDE THE CASING AND FLOW CAPACITY

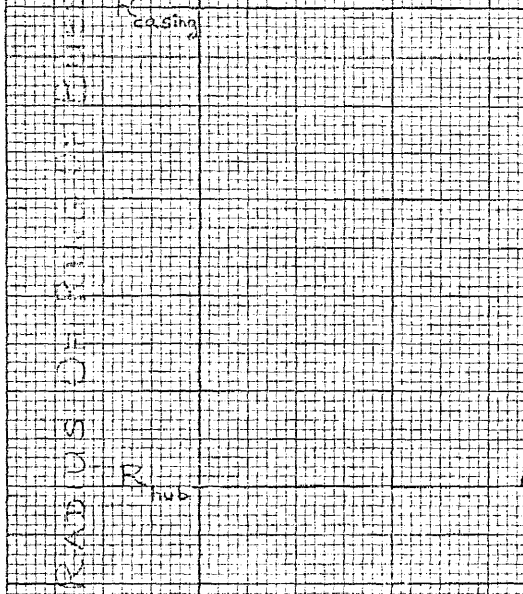

NOTE: THERE WAS NO NOTICEABLE EFFECT OF PUMP SPEED ON THE RADIUS OF RING OF BUBBLES.

CAPACITY

36 GPM (max. flow)

FIGURE 17A

A SYMBOLIC DIAGRAM OF THE APPARATUS

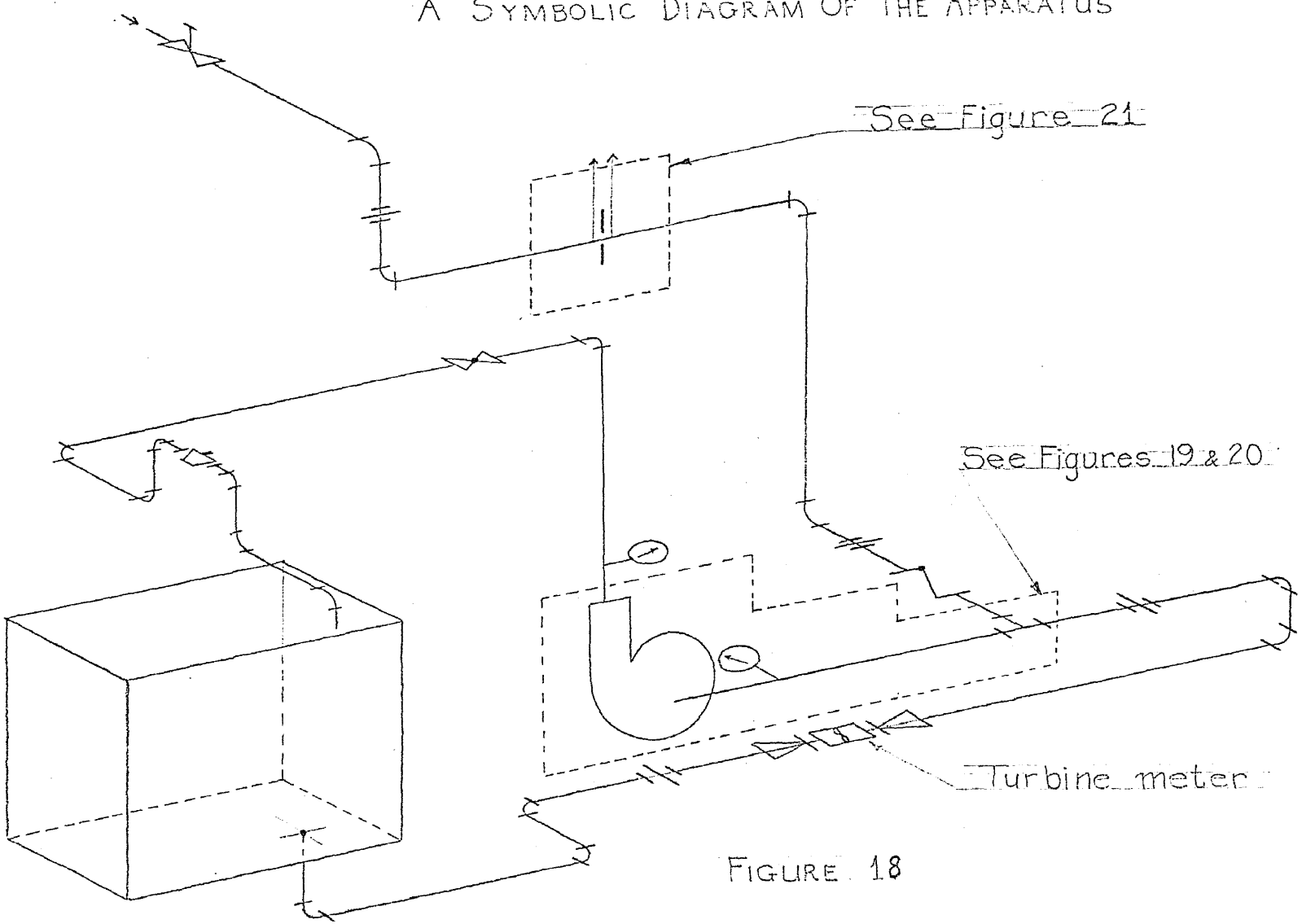

FIGURE 18

PUMP CASING & IMPELLER

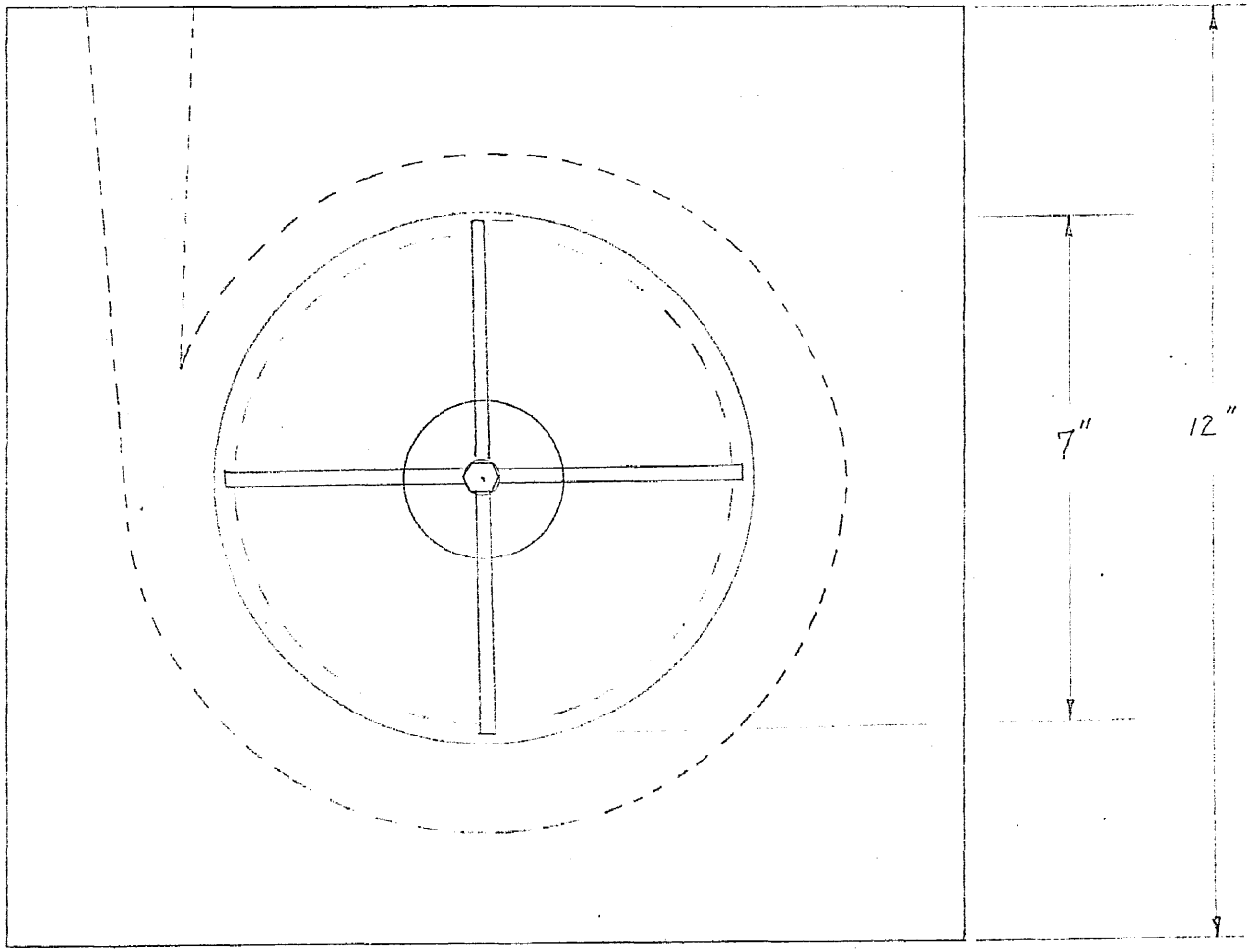

FIGURE 19

Scale: 1 : 2.4 in.

THE AIR-INJECTION SYSTEM

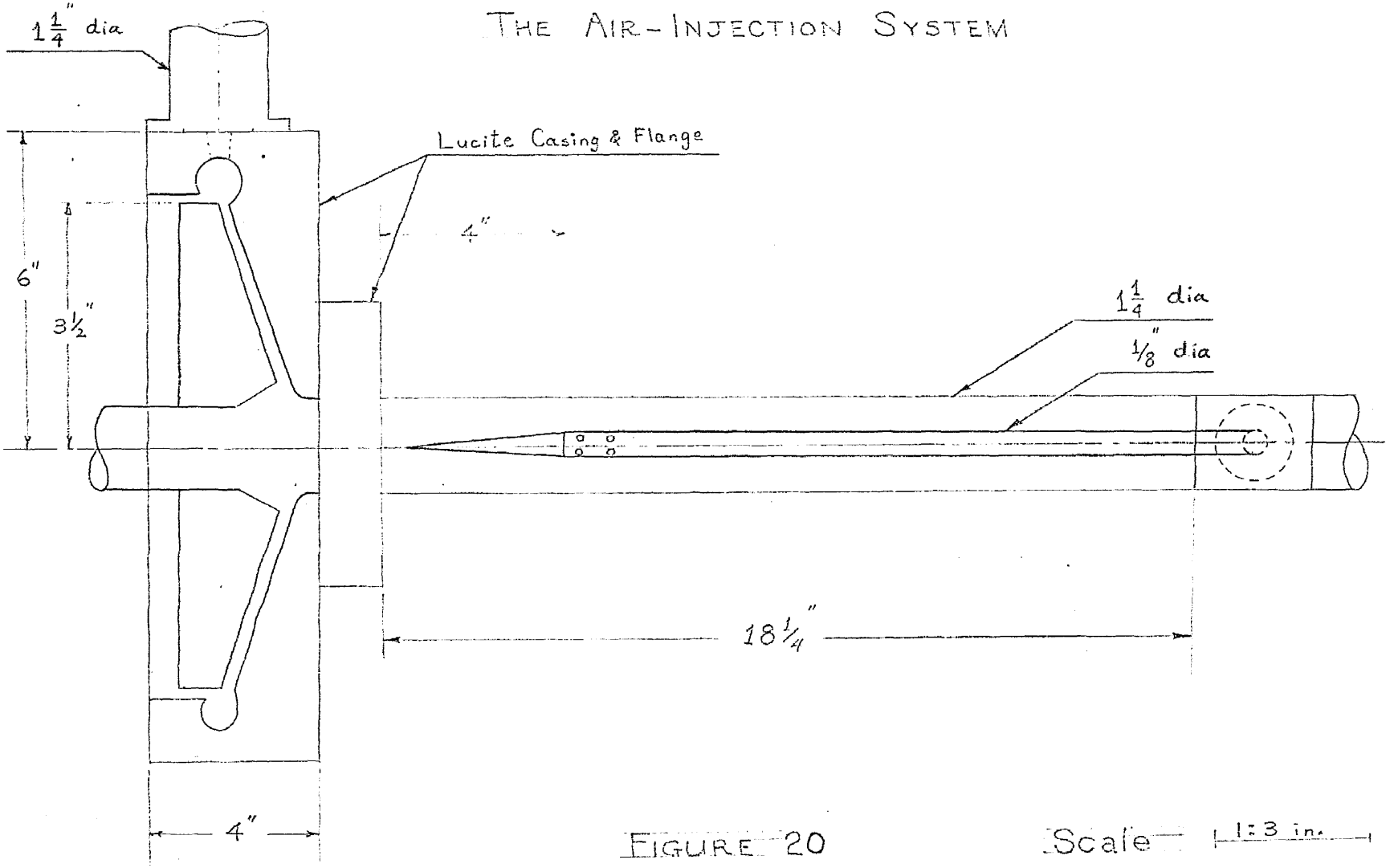

FIGURE 20

Scale 1:3 in.

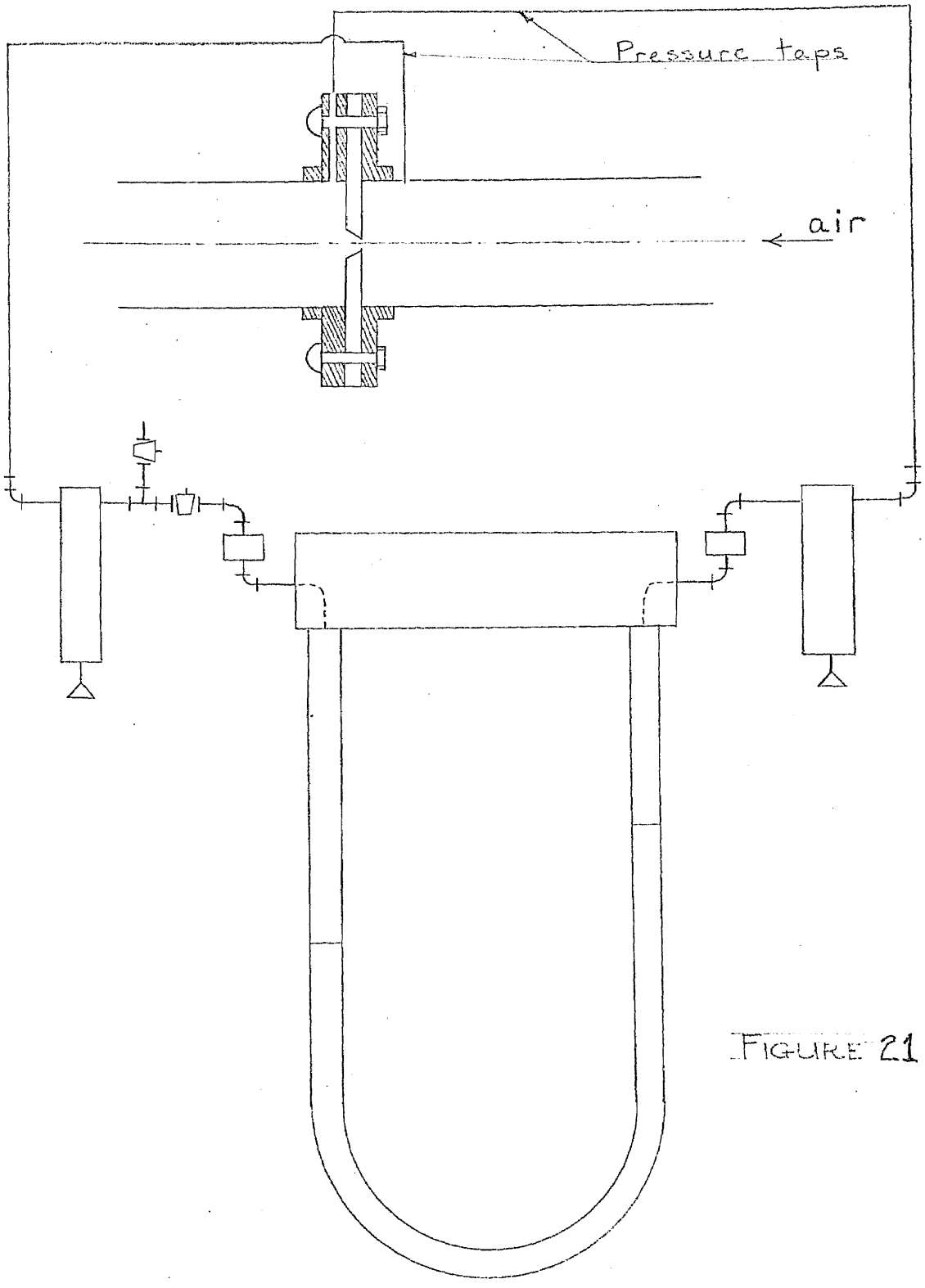

FIGURE 21

THE ORIFICE & THE AIR FLOW MEASURING UNIT

An Illustration of the
Helical Streamline with traped air bubbles

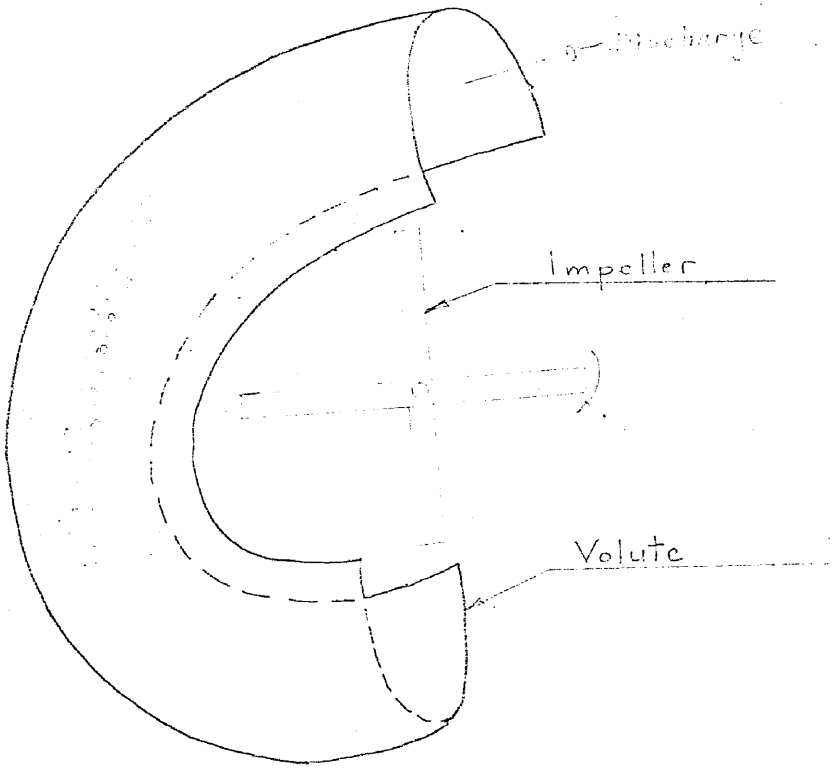

FIGURE 22

CALIBRATION OF SUCTION POTTERMETER

Counts/Sec.	GPM
56	5.03
69	5.59
87	7.30
91	8.40
123	10.83
146	12.97
160	13.72
179	15.37
191	17.20
192	17.90
196	18.45
224	20.25
227	20.75
244	22.25
247	22.7
265	24.0
267	24.9

CALIBRATION OF ORIFICE

$$w_h = 1.03\sqrt{h_{Hg}}$$

Inches of Hg	w_h (lb_m of air/ hr.)
0.0	0.00
0.5	0.73
1.0	1.00
1.5	1.25
2.0	1.45
2.5	1.63
3.0	1.78
3.5	1.91
4.0	2.06
4.5	2.18
5.0	2.30
6.0	2.52
7.0	2.72
8.0	2.91
9.0	3.09
10.0	3.26
12.0	3.56
15.0	3.99
20.0	4.61
25.0	5.15
30.0	5.63
35.0	6.09
40.0	6.47

THE CONVERSION OF THE PRESSURE DIFFEREINTIAL ACROSS THE ORIFICE TO FT^3/SEC. OF AIR.

P"Hg.	Air Flow(^{lbm}/hr)*	Air Flow(ft^3/sec.)
0.2	0.45	1.4×10^{-3}
0.3	0.55	1.72×10^{-3}
0.4	0.65	2.03×10^{-3}
0.5	0.70	2.18×10^{-3}
0.6	0.75	2.34×10^{-3}
0.65	0.80	2.50×10^{-3}
0.70	0.85	2.65×10^{-3}
0.80	0.90	2.81×10^{-3}

* Obtained from Orifice calibration curve.

TABULATED DATA

3500 RPM

Flow Capacity (GPM)	Discharge Pressure (ft.)	Suction Pressure (ft.)	Brake Horse Power	Efficiency	Air Flow (10^3 ft^3/sec)
36	9.25	33.4	3.53	2.38	0
35	175	26.6	4.87	31.9	
28.7	182	22.1	4.8	27.6	
20.7	196	13	4.4	23.3	
13.7	203	6.24	4.07	17.3	
8.0	208	2.83	3.8	11.1	
3.0	208	1.13	3.53	4.48	
36	9.25	33.4	3.47	2.43	1.4
33.5	178	26.1	5.14	29.3	
29	184	22.7	5.0	27.1	
23.8	192	16.4	4.8	24.1	
19.4	196	11.3	4.67	20.6	
14	203	6.8	4.2	17.1	
7	208	2.27	3.67	10.0	
37	9.25	30.6	3.33	2.6	1.72
36	162	28.3	5.20	28.3	
32.4	201	23.8	5.27	31.1	
27	198	20.4	5.27	25.5	
22	215	13.6	5.07	23.6	
19	205	9.64	4.94	19.9	
14	194	6.24	4.6	14.9	
7.7	171	2.27	4.26	7.7	
37	11.5	29.5	3.53	3.04	2.18
36	74	27.8	4.6	14.7	
31	129	23.8	5.2	19.5	
26.6	162	20.4	5.07	21.5	
20	189	11.3	4.94	18.4	
12.3	129	4.53	3.87	10.3	
7	65	1.13	2.13	5.4	
24.4	9.25	17.0	2.33	2.45	2.65
18.2	23.1	11.3	2.13	5.0	
14.7	16.2	5.64	1.33	4.52	
—	—	—	—	—	

TABULATED DATA

3000 RPM

GPM	Disch.head (pt)	P_s(ft)	b^{hp}	EFF.	Air-Flow (10^{-3} $\frac{ft^3}{sec}$)
36	9.25	33.4	2.86	2.94	0
32.5	132	24.9	3.48	31.2	
27.7	136	21.5	3.37	28.3	
21.7	146	13.6	3.26	24.6	
18.3	150	10.2	3.03	22.9	
13.5	153	5.67	2.86	18.3	
7.2	155	2.27	2.57	11.0	
36	9.25	33.4	2.86	2.94	1.4
31.5	129	24.9	3.48	29.6	
27.0	134	20.4	3.43	26.6	
21.7	143	13.6	3.20	24.5	
18.5	148	10.2	3.03	22.8	
14	153	6.8	2.97	18.2	
9	155	2.84	2.8	12.6	
36	9.25	32.3	2.86	2.94	1.72
29.7	129	23.8	3.54	27.3	
26	125	19.3	3.37	24.4	
19.2	146	11.3	3.14	22.5	
14.3	150	6.8	2.97	18.2	
6.8	150	2.27	2.68	9.61	
36	9.25	32.3	2.86	2.84	2.18
29.7	120	22.7	3.43	26.3	
22.5	139	14.7	3.32	23.8	
19.3	122	10.2	3.14	19.0	
14.7	113	6.8	2.91	14.4	
9.0	102	2.83	2.46	9.46	
6.7	46	2.27	1.83	4.25	
36	9.25	27.4	2.68	3.14	2.50
32.4	23.1	24.9	2.74	6.91	
22.5	53.5	13.6	2.46	12.4	
19	81.	7.36	2.63	15.5	
11.7	39.3	4.53	2.00	5.82	
6.3	6.9	1.13	.57	1.9	
35	9.25	26.6	2.57	3.19	2.65
32.2	16.2	25.04	2.63	5.0	
—	—	—	—	—	

TABULATED DATA

2500 RPM

GPM	P_d(ft)	P_s(ft)	b^{hp}	EFF.	Air Flow (10^{-3} $\frac{ft^3}{sec}$)
36	11.5	31.2	2.24	4.7	0
33.25	78.5	22.1	2.67	24.8	
28.8	83.2	19.3	2.72	22.3	
21.4	97.0	11.33	2.29	23.0	
15	106.0	5.66	2.00	20.1	
8.5	109.0	2.26	1.81	13.2	
36	9.25	32.9	2.24	3.77	1.72
32.2	85.5	23.8	2.62	26.6	
27.8	90.1	20.4	2.48	25.6	
21.5	97.1	12.5	2.24	23.6	
14.5	104.0	6.24	1.95	19.6	
9.0	108.5	2.27	1.72	14.4	
36	9.25	32.9	2.24	3.74	2.03
35	83.2	25.5	2.57	27.6	
28	86.8	20.4	2.38	25.8	
23.7	94.7	14.75	2.24	25.3	
17	101.5	7.95	2.00	21.8	
10	108.5	2.84	1.72	15.9	
36	9.25	31.2	2.33	3.62	2.34
31.5	85.5	22.1	2.57	26.6	
25.2	92.50	17.6	2.33	25.3	
21.6	86.8	11.3	2.24	21.2	
13.5	99.4	4.54	1.90	17.9	
5.4	83.1	0	1.53	7.41	
36	9.25	29.0	2.24	3.77	2.50
27	60.0	17.0	2.43	16.9	
24.1	46.2	13.6	2.24	12.6	
17	39.3	6.8	1.81	9.34	
9.0	18.5	0.57	1.00	4.22	
18.6	2.81	9.1	1.29	0.84	2.65
15.3	6.93	6.25	1.14	2.35	
10.8	13.85	1.13	1.05	3.59	

TABULATED DATA

2000 RPM

GPM	P_D (ft)	Ps (ft)	bhp	EFF.	Air Flow (10^{-3} $\frac{ft^3}{sec}$)
36	13.9	25	1.60	7.92	0
35	23.1	22.6	1.64	12.5	
29.7	37.0	19.8	1.64	17.0	
23.8	48.5	13.6	1.525	19.2	
18.3	60.0	7.95	1.258	22.1	
12	67.0	2.84	1.068	19.0	
6	69.3	0.	0.954	11.0	
36	11.5	28.1	1.64	6.4	1.4
30.7	46.2	22.0	1.45	24.7	
26.2	50.1	18.1	1.37	24.3	
21	60.0	11.9	1.29	24.7	
15.4	64.7	5.7	1.18	21.4	
9.6	67.0	2.3	1.07	15.2	
31	11.5	21.6	1.485	6.1	1.72
27	20.8	17.6	1.41	10.1	
24.3	25.4	14.5	1.37	11.4	
20	32.4	9.1	1.18	13.9	
14	25.4	3.4	0.80	11.25	
27	9.25	18.1	1.295	4.9	2.03
23.3	13.9	13.6	1.22	6.7	
20	13.9	7.95	.99	7.1	
13.5	4.62	1.7	.76	2.1	
7.2	2.31	0	.68	0.6	
25.6	9.25	17.6	1.26	4.75	2.18
20.7	13.9	9.65	1.07	6.8	
16.2	9.25	4.55	0.80	4.75	
7.2	2.31	0	0.57	0.7	
22.5	9.25	13.6	1.18	4.45	2.34
18	4.62	1.1	0.725	2.9	

TABULATED DATA

1500 RPM

GPM	P_D (ft)	P_S (ft)	b^{hp}	EFF.	Air Flow (10^{-3} $\frac{ft^3}{sec}$)
28	9.25	17	0.944	6.93	0
20.5	23.10	10.2	0.886	13.5	↓
16.2	31.20	6.24	0.657	19.5	
13.5	34.70	3.97	0.629	18.8	
7.2	39.30	.57	0.549	13	
31	11.5	22	0.80	11.3	1.4
26	18.5	18.1	0.74	16.4	↓
20.5	26.6	11.3	0.66	20.9	
15.7	32.4	6.2	0.60	21.5	
9.4	37.0	1.7	0.51	17.2	
5.0	38.2	0	0.49	9.9	
28	11.5	20.5	0.94	8.7	1.72
24.5	23.1	15.3	0.885	16.2	↓
17.5	25.4	7.9	0.83	13.6	
14.4	18.5	5.1	0.77	6.8	
12.2	16.2	3.4	0.74	6.8	
7.7	13.9	1.1	0.66	4.1	
25.6	9.25	17.6	0.86	6.95	2.18
20.7	17.3	10.8	1.77	11.8	↓
17.7	25.4	7.4	0.685	16.6	
11.7	13.9	2.8	0.54	7.60	
6.4	6.9	1.1	0.49	2.3	
22.7	6.9	13.0	0.77	5.2	2.65
19	10.4	9.1	0.685	7.3	↓
16.2	13.9	6.2	0.63	9.1	
9.2	5.78	1.7	0.46	2.9	
17.2	4.62	7.9	0.66	3.04	2.81

CALCULATIONS

1. DETERMINATION OF VOLUMETRIC AIR FLOW RATE:

Density of air at ambient conditions, $\rho = \frac{P}{RT}$

where P = 14.7 psia
R = 53.35 ft.lb_f/ lb_m-R
T = 78 °F

$$\rho = \frac{14.716_f}{in^2} \times \frac{144\ in^2}{ft^2} \times \frac{1}{(53.35\ ft\text{-}lb_f)(538\ ^\circ R)} \frac{lbm\text{-}^\circ R}{}$$

$$\rho = 7.38 \times 10^{-2}\ (lb_m/ ft^3)$$

A Sample Calculation

Gage Pressure at Orifice = 3 psig (Constant).

Air Density at Orifice $= (7.38 \times 10^{-2}) \frac{(14.7 + 3)}{14.7}$

$= 8.9 \times 10^{-2}\ lb_m/ft^3$

Air Flow Rate = $0.45^*\ lb_m \times \frac{1\ hr}{3600\ sec} \times \frac{ft^3}{8.9 \times 10^{-2}\ lb_m}$

$= 1.4 \times 10^{-3}\ ft^3/sec$

* This is the mass flow rate corresponding to a pressure differential of 0.2 "Hg obtained from the orifice calibration curve.

CALCULATIONS

2. DETERMINATION OF MAX. DISCHARGE & SUCTION PRESSURES:

(Based on Manufacturer's data)

$$250 = \frac{PSI \times 2.31}{1}$$

MAX. DISCH. PRESSURE = 110 psi

$$15 = \frac{PSI \times 2.31}{1}$$

MAX. SUCTION = 6.5 psi

---

3. DETERMINATION OF AIR FLOW RATE THRU 1"-PIPE BY MEANS OR AN ORIFICE:*

$W_h = 359\ CFd^2F_a Y\sqrt{h_w/v_1} = 359\ Kd^2 Y\sqrt{h_w/v_1}$ ..(i) where

w_h = Weight flow rate, lbs/hr

C = Coefficient of discharge

F = Velocity of approach factor = $\frac{1}{\sqrt{1-\beta^4}}$

β = Ratio of orifice throat to pipe J.D.

d = Orifice throat diameter, inches

F_a = Factor accounting for thermal expansion of orifice

Y = Net expansion factor

---

* POWER TEST CODE - FLOW MEASUREMENT p.57

h_w = Differential pressure, inches of water at 68°F

v_1 = Specific volume of air at inlet of orifice $\frac{\text{cu.ft}}{\text{lb}}$

β = 0.357/1.049 = 0.34

$F = \frac{1}{\sqrt{1-\beta^4}}$ = $\frac{1}{\sqrt{1-0.01336}}$ = 1.00965

$d^2 = (0.357 \text{ in})^2 = 0.1275 \text{ in}^2$

$F_a \approx 1.0$

$g\mu|_{68°F} = 0.000012 \frac{\text{lbf}}{\text{ft.sec.}} = 3.8 \times 10^{-7} \frac{\text{lbf - sec}}{\text{ft}^2} \times 32 \frac{\text{ft}}{\text{sec}^2}$

$R_e = \frac{VD\gamma}{g\mu}$

The term K in equation (i) above is determined by the Reynold's No which doesn't have a considerable bearing upon it.

Therefore, the following assumption is made:-

(1) V = 10 ft/sec (approx.)

Also D = 1.049 x 1/12 = 0,0874 ft

γ = 0.075

$g\mu$ = 0.0000121

$W_h = 359 Kd^2 = 359 Kd^2$

Assume (1) ΔP = 6 in Hg β = 0.34

(2) P_1 = 25 psig

(3) T = 70°F
= 460 + 70 d = 0.357 in
= 530°R

$P\upsilon = RT$

$\upsilon_1 = \frac{RT}{P_1} = \frac{(53.35)(530)}{(39.7)\ 144} = \frac{(53.35)(530)}{(144)\ (39.7)} = 49.4\ \frac{ft^3}{lb_m}$

$h_w = 6\ \text{inHg} \times 13.6\ \frac{\text{in Water}}{\text{in Hg}} = 81.6\ \text{in.H}_2\text{O}$

$d^2 = 0.1275\ \text{in}^2$

$h_w/p_1 = 2.06$

$Y|_{FIG\ 40\ \beta\ \beta = 0.34} = 0.97$

Assume K = 0.601 Assuming that $R_e \approx 10^6$, and since R_e does not have a critical effect on K , this is a safe assumption. But the variation of Y with h_w is negligible

In the equation

$W_h = 359\ Kd^2\ Y\sqrt{h_w/\upsilon_1}$ assuming 1. P_1 = 25psig

2. T = 70°F

3. V ≈ 10ft/sec

Throughout the exp.

W_h = Constant $\sqrt{h_w}$

$= (359)(0.601)(0.1275)(0.970)\left(\frac{1}{\sqrt{49.4}}\right)\sqrt{h_w}$

(A)..... $\boxed{W_h = 3.8\sqrt{h_w}}$

$= 3.8\sqrt{(h_w\ \text{in}\ H_2O)\frac{1\ \text{in Hg}}{13.6\ \text{in}\ H_2O}} = \frac{3.8}{\sqrt{13.6}}\sqrt{h_w\ \text{inch Hg}}$

(B)... $\boxed{w_h = 1.03\sqrt{h_{wg}}}$ See Pages 54 and 46 for tabulation and plot.

---

4. EQUATIONS USED TO CALCULATE PERFORMANCE PARAMETERS:

1.- GPM : (Use Calibration Curve to Convert Electronic Counts/sec to GPM).

2.- Discharge Head, P_D:

$$P_D(\text{ft.}) = P_D(\text{PSI}) \times 2.31$$

3.- Suction Head, P_s;

$$P_s(\text{ft.}) = P_s(\text{"Hg"}) \times 1.133$$

4.- Brake Horse Power, bhp:

$$\text{bhp} = \frac{Lr\omega}{63025}$$

5.- Efficiency, η % :

$$\eta = \frac{Q\gamma H}{550\ \text{bhp}}$$

5. DETERMINATION OF MINIMUM No OF PICTURES PER SECOND OF ROTATING IMPELLER: -

Pictures per second (pps) $= \left(\frac{1}{20}\right)\left(N\right)\left(\omega\right)$

Where N = No. of impeller blades

ω = Impeller rpm

For this configuration N = 4 blades

and ω = 1500, 2000, 2500, 3000, 3550 rpm

Impeller RPM	Minimum PPS
1500	300
2000	400
2500	500
3000	600
3500	700

CHARACTERISTICS OF APPARATUS:

A.- DYNAMOMETER

7.5 HP
250 Volts
800-- 4000 RPM (variable)
25 - 28 Amps

B.- RESERVOIR

Capacity 67.5 cu.ft = 500 gal.

C.- PIPING

	Nominal	I.D.	O.D.
Air Line	1"	1.049"	1.315"
Water "	1¼"	1.380"	1.660"

DATA

RPM Tach	RPM Strob	Water Flow Counts/sec	Air Flow "Hg" L	Air Flow "Hg" R	Disch. Pressure Psig	Suction Pressure "Hg"	Force on Torque bar lb.
3500	3740	404	0	0	4	29.5	5.3
		390	0	0	76	23.5	7.3
		320	0	0	79	19.5	7.2
		239	0	0	85	11.5	6.6
		153	0	0	88	5.5	5.7
		90	0	0	90	2.5	5.7
		28	0	0	90	1.0	5.3
		405	-.1	+.1	4	29.5	5.2
		375	-.1	+.1	77	23	7.7
		323	-.1	+.1	80	20	7.5
		265	-.1	+.1	83	14.5	7.2
		215	-.1	+.1	85	10	7.0
		157	-.1	+.1	88	6	6.2
		78	-.1	+.1	90	2	5.5
		408	-.15	+.15	4	27	5.0
		406	-.15	+.15	70	25	7.8
		360	-.15	+.15	87	21	7.9
		300	-.15	+.15	86	18	7.9
		244	-.15	+.15	93	12	7.6
		209	-.15	+.15	89	8.5	7.4
		155	-.15	+.15	84	5.5	6.9
		86	-.15	+.15	74	2.0	6.4
		407	-.25	+.25	5	26	5.3
		406	-.25	+.25	32	24.5	6.9
		345	-.25	+.25	56	21	7.8
		296	-.25	+.25	70	18	7.6
		223	-.25	+.25	82	10	7.4
		137	-.25	+.25	56	4	5.8
		76	-.25	+.25	28	1	3.2
		271	-.35	+.35	4	15	3.5
		202	-.35	+.35	10	10	3.2
		163	-.35	+.35	7	5	2.0
		Unavaible					

Torque arm= 11.994; Air Reservoir Pressure= 25 psig
Air Temp.= 78 F°

DATA

RPM Tach	RPM Strob	Water Flow Counts/sec	Air Flow "Hg" L	Air Flow "Hg" R	Disch. Pressure Psig	Suction Pressure "Hg"	Force on Torque bar lb.
3000	3170	404	0	0	4	29.5	5.0
		362	0	0	57	22	6.1
		308	0	0	59	19	5.9
		241	0	0	63	12	5.7
		204	0	0	65	9	5.3
		150	0	0	66	5	5.0
		80	0	0	67	2	4.5
		403	-.1	+.1	4	29.5	5.0
		351	-.1	+.1	56	22	6.1
		300	-.1	+.1	58	18	6.0
		242	-.1	+.1	62	12	5.6
		205	-.1	+.1	64	9	5.3
		157	-.1	+.1	66	6	5.2
		99	-.1	+.1	67	2.5	4.9
		404	-.15	+.15	4	28.5	5.0
		330	-.15	+.15	56	21	6.2
		290	-.15	+.15	54	17	5.9
		213	-.15	+.15	63	10	5.5
		159	-.15	+.15	65	6	5.2
		76	-.15	+.15	65	2	4.7
		405	-.25	+.25	4	28.5	5.0
		330	-.25	+.25	52	20	6.0
		250	-.25	+.25	60	13	5.8
		214	-.25	+.25	53	9	5.5
		163	-.25	+.25	49	6	5.1
		100	-.25	+.25	44	2.5	4.3
		75	-.25	+.25	20	2	3.2
		404	-.325	+.325	4	24.2	4.7
		360	-.325	+.325	10	22	4.8
		250	-.325	+.325	23	12	4.3
		210	-.325	+.325	35	6.5	4.6
		130	-.325	+.325	17	4	3.5
		70	-.325	+.325	3	1	1.0
		388	-.35	+.35	4	23.5	4.5
		360	-.35	+.35	7	22.0	4.6

Torque Arm= 11.994 in; Air Reservoir Press= 25 psig
Air Temp= 78 F°

DATA

RPM Tach	RPM Strob	Water Flow Counts/sec	Air Flow "Hg" L	Air Flow "Hg" R	Disch. Pressure Psig	Suction Pressure "Hg"	Force on Torque bar lb
2500	2590	406	0	0	5	27.5	4.7
		370	0	0	34	19.5	5.6
		320	0	0	36	17.0	5.7
		240	0	0	42	10.0	4.8
		165	0	0	46	5	4.2
		95	0	0	47	2	3.8
		430	-.15	+.15	4	29	4.7
		358	-.15	+.15	37	21	5.5
		309	-.15	+.15	39	18	5.2
		238	-.15	+.15	42	11	4.7
		162	-.15	+.15	45	5.5	4.1
		100	-.15	+.15	47	2.0	3.6
		404	-.20	+.20	4	29	4.7
		390	-.20	+.20	36	22.5	5.4
		313	-.20	+.20	38	18	5.0
		264	-.20	+.20	41	13	4.7
		190	-.20	+.20	44	7	4.2
		110	-.20	+.20	47	2.5	3.6
		402	-.30	+.30	4	27.5	4.9
		350	-.30	+.30	37	19.5	5.4
		280	-.30	+.30	40	15.5	4.9
		240	-.30	+.30	38	10.0	4.7
		150	-.30	+.30	43	4.0	4.0
		60	-.30	+.30	36	0	3.2
		403	-.325	+.325	4	25.5	4.7
		300	-.325	+.325	26	15.0	5.1
		269	-.325	+.325	20	12	4.7
		190	-.325	+.325	17	6	3.8
		100	-.325	+.325	8	0.5	2.1
		207	-.35	+.35	1	8	2.7
		170	-.35	+.35	3	5.5	2.4
		120	-.35	+.35	6	1	2.2

Unavailable

Torque Arm= 11.994 in; Air Reservoir= 25psig

Air Temp= 78 F°

DATA

RPM Tach	RPM Strob	Water Flow Counts/sec	Air Flow "Hg" L	Air Flow "Hg" R	Disch. Pressure Psig	Suction Pressure "Hg"	Force on Torque bar lb
2000	2050	404	0	0	6	22	4.2
		388	0	0	10	20	4.3
		325	0	0	16	17.5	4.3
		265	0	0	21	12	4.0
		204	0	0	26	7	3.3
		133	0	0	29	2.5	2.8
		67	0	0	30	0	2.5
		400	-.1	+.1	5.0	24.8	4.3
		342	-.1	+.1	20.0	19.4	3.8
		292	-.1	+.1	22.0	16.0	3.6
		234	-.1	+.1	26	10.5	3.4
		171	-.1	+.1	28	5.0	3.1
		107	-.1	+.1	29	2.0	2.8
		344	-.15	+.15	5	19	3.9
		300	-.15	+.15	9	15.5	3.8
		270	-.15	+.15	11	12.8	3.7
		220	-.15	+.15	14	8.0	3.1
		156	-.15	+.15	11	3.0	2.1
		Unavailable			0		
		300	-.2	+.2	4	16	3.4
		260	-.2	+.2	6	12	3.2
		220	-.2	+.2	6	7	2.6
		150	-.2	+.2	2	1.5	2.0
		80	-.2	+.2	1	0	1.8
		Unavailable					
		285	-.25	+.25	4	15.5	3.3
		230	-.25	+.25	6	8.5	2.8
		180	-.25	+.25	4	4	2.1
		80	-.25	+.25	1	0	1.5
		Unavailable					
		250	-.30	+.30	4	12	3.1
		200	-.30	+.30	2	1	1.9
		Unavailable					

Torque Arm= 11.994 in ; Air Reservoir Press.= 25psig
Air Temp.= 78 F^{0}

DATA

RPM Tach	RPM Strob	Water Flow Counts/sec	Air Flow "Hg" L	Air Flow "Hg" R	Disch. Pressure Psig	Suction Pressure "Hg"	Force on Torque bar lb.
1500	1500	310	0	0	4	15	3.3
		226	0	0	10	9	3.1
		180	0	0	13.5	5.5	2.3
		150	0	0	15	3.5	2.2
		80	0	0	17	0.5	1.9
		342	-.1	+.1	5	19.4	2.8
		290	-.1	+.1	8	16.0	2.6
		228	-.1	+.1	11.5	10.0	2.3
		174	-.1	+.1	14.0	5.5	2.1
		106	-.1	+.1	16.0	1.5	1.8
		54	-.1	+.1	16.5	0	1.7
		314	-.15	+.15	5	18.1	3.3
		217	-.15	+.15	10	13.5	3.1
		196	-.15	+.15	11	7.0	2.9
		160	-.15	+.15	8	4.5	2.7
		136	-.15	+15	7	3.0	2.6
		86	-.15	+.15	6	1.0	2.3
		285	-.25	+.25	4	15.5	3.0
		230	-.25	+.25	7.5	9.5	2.7
		197	-.25	+.25	11	6.5	2.4
		130	-.25	+.25	6	2.5	1.9
		71	-.25	+.25	3	1.0	1.7
		Unavailable					
		252	-.35	+.35	3	11.5	2.7
		210	-.35	+.35	4.5	8	2.4
		180	-.35	+.35	6	5.5	2.2
		103	-.35	+.35	2.5	1.5	1.6
		Unavailable					
		192	-.4	+.4	2.0	7.0	2.3

Torque Arm= 11.994 in; Air Reservoir Press= 25 psig
Air Temp= 78 F°

CALIBRATION DATA OF SUCTION POTTERMETER

RPM (tach)	RPM (Strob)	Counts / sec.	Wt. of Water (Lb.)	Time int (Sec)
800	823	69	50	64.2
1000	1012	87	50	49.2
1410	1400	123	50	33.15
1800	1770	160	50	26.17
2000	1980	179	50	23.32
2200	2170	196	50	19.46
2490	2448	227	50	17.28
2700	2643	244	70	22.6
2900	2830	265	70	20.86

LIST OF REFERENCES

(1) Stepanoff, A.J. Pumps and Blowers-Two Phase Flow. New York: John Wiley and Sons, 1966

(2) Arbiter, N., Harris, C.C., and Yap, R.F. "Hydrodynamics of Floatation Cells." Henry Krumb School of Mines, Columbia University, New York, 1968

(3) Biheller, W. "Air Handling Capability of Centrifugal Pumps." Worthington Corporation Research Paper. Harrison, N.J. 1957

(4) Boyce, M.P. "A Practical Three-Dimensional Flow Visualization Approach to the Complex Flow Characteristics in a Centrifugal Impeller," Curtiss-Wright Corporation, Wood-Ridge, N.J. 1966